Quantification of GR effects in muon g-2, EDM and other spin precession experiments

András László

Wigner Research Centre for Physics, Budapest

E-mail: `laszlo.andras@wigner.mta.hu`

Zoltán Zimborás

Wigner Research Centre for Physics, Budapest

E-mail: `zimboras.zoltan@wigner.mta.hu`

Abstract. Recently, Morishima, Futamase and Shimizu published a series of manuscripts, putting forward arguments, based on a post-Newtonian approximative calculation, that there can be a sizable general relativistic (GR) correction in the experimental determination of the muon magnetic moment based on spin precession, i.e., in muon g-2 experiments. In response, other authors argued that the effect must be much smaller than claimed. Further authors argued that the effect exactly cancels. Also, the known formulae for de Sitter and Lense-Thirring effect do not apply due to the non-geodesic motion. All this indicates that it is difficult to estimate from first principles the influence of GR corrections in the problem of spin propagation. Therefore, in this paper we present a full general relativistic calculation in order to quantify this effect. The main methodology is the purely differential geometrical tool of Fermi-Walker transport over a Schwarzschild background. Also the Larmor precession due to the propagation in the electromagnetic field of the experimental apparatus is included. For the muon g-2 experiments the GR correction turns out to be very small, well below the present sensitivity. However, in other similar storage ring experimental settings, such as electric dipole moment (EDM) search experiments, where the so-called frozen spin method is used, GR gives a well detectable effect, and should be corrected for. All frozen spin scenarios are affected which intend to reach a sensitivity of 0.1 microradians/second for the spin precession in the vertical plane.

1. Introduction

In a recent series of papers [1, 2, 3], it was claimed that, in the muon anomalous magnetic moment experiments [4, 5, 6, 7], there can be a general relativistic (GR) correction to the precession effect of the muon spin direction vector when orbiting in the magnetic storage ring sitting on the Earth's surface in a Schwarzschild metric. These calculations were based on a post-Newtonian approximation, and the authors claimed that the pertinent effect may cause an unaccounted systematic error in the measurement of the muon's anomalous magnetic moment, often referred to as g-2. Other papers [8, 9] responded that the effect is much smaller. Further papers [10] responded that the effect exactly cancels. Moreover, the usual formulae of de Sitter and Lense-Thirring precession [11] do not apply, since the pertinent orbit is non-geodesic. All this suggests that it is relatively difficult to say something from first principles on the magnitude of GR corrections for spin transport in a gyroscopic motion along a forced orbit. Motivated by these, in the present paper, we intend to quantify the pertinent effect in the context of GR. We use the differential geometrical tool of Fermi-Walker transport of vectors along trajectories in spacetime. In this way, the kinematic precession, called the Thomas precession, can be quantified over the Schwarzschild background field of the Earth. This is then compared to the Minkowski limit, i.e., when GR is neglected. The effect of the Larmor precession in the electromagnetic field of the experimental setting is also quantified, and its corresponding GR correction is also evaluated. The calculations show that the GR corrections for the actual g-2 experimental setting [4, 5, 6, 7] is very small, well below the experimental sensitivity. There are, however, other spin precession experiments, such as the electric dipole moment (EDM) search experiments [12, 13, 14], where it turns out that GR gives a rather large signal. Since these experiments are intended as sensitive probes for Beyond Standard Model (BSM) scenarios, their experimental data should be corrected for the GR effect. In particular, the EDM experiments [12, 13, 14] could be thought of also as sensitive GR experiments on spin propagation of elementary particles, kind of microscopic versions of Gravity Probe B [15, 16] gyroscope experiment. During the past years there have been a few papers warning about the possibility of such an effect [17, 18, 19, 20, 21]. These estimations, however, are not fully covariant Lorentz geometric GR calculations, but are mostly special relativistic or semi-general relativistic, or applying other kind of approximations such as not fully taking into account GR for the electrodynamic part. As a result, the estimations [17, 18, 19, 20] differ from our geometric GR calculation in the details of the particle velocity dependence, and with some factors. The post-Newtonian estimation of [21], where the GR effect for the special case of a purely electric frozen spin storage ring is quantified, is confirmed by our covariant calculations. Since the EDM signal is expected to sit on this large GR background of the order of 30 nrad/sec, the pertinent factors matter a lot for discrimination from a BSM signature with the planned precision of 1 nrad/sec. The GR signal, however, can also be disentangled from a true EDM signal due to their opposite space reflection behavior, i.e., by switching beam direction.

The structure of the paper is as follows. Section 2 outlines the kinematic setting of our model of the experimental situation. In Section 3 and 4, we discuss, from a geometrical point of view, the Fermi-Walker transport (gyroscopic equation) and the general relativistic Thomas precession, respectively. The GR corrections to the Thomas precession is evaluated in Section 5. In Section 6, the idealized model of electromagnetic fields in an electromagnetic storage ring over a Schwarzschild background is outlined, and their Fermi-Walker-Larmor spin transport is evaluated in Section 7. The analytical formulae are derived for a combined Thomas and Larmor precession over the Schwarzschild background in Section 8. Finally, in Section 9 the total GR corrections are evaluated, which is followed by our concluding remarks in Section 10.

2. The kinematic setting

The kinematic setting of the experiment is outlined in Fig. 1. The gravitational field of the Earth is modelled by a Schwarzschild metric with r_S being the corresponding Schwarzschild radius, $r_S = \frac{2MG}{c^2}$. The non-sphericity of the Earth as well as its rotation is neglected. We use the standard Schwarzschild coordinates t, r, ϑ, φ, and thus the components of the Schwarzschild metric read as:

$$g_{\mathsf{ab}}(t, r, \vartheta, \varphi) = \begin{pmatrix} 1 - \frac{r_S}{r} & 0 & 0 & 0 \\ 0 & -\frac{1}{1-\frac{r_S}{r}} & 0 & 0 \\ 0 & 0 & -r^2 & 0 \\ 0 & 0 & 0 & -r^2 \sin^2 \vartheta \end{pmatrix}. \tag{1}$$

In such coordinates, the Earth's surface is at an $r = \text{const}$ level-surface, we denote this radius by R. By convention, the North pole of the spherical coordinates is adjusted such that it corresponds to the central axis of the storage ring, i.e., this axis is at $\vartheta = 0$. The entire storage ring is located at an $r = R$, $\vartheta = \text{const}$ surface, where the corresponding ϑ coordinate value is denoted by Θ. The radius of the storage ring is then $L = R \sin \Theta$. Throughout the paper, the coordinate indices are denoted by fonts like $\mathsf{a}, \mathsf{b}, \mathsf{c}, \dots$ and take their value from the index set $\{0, 1, 2, 3\}$. Occasionally, the alternative notation $\{t, r, \vartheta, \varphi\}$ is used as equivalent symbols for the indices $\{0, 1, 2, 3\}$. Moreover, we will also use the Penrose abstract indices [23], with index symbol fonts like $a, b, c, \dots$ in order to aid the notation of various tensorial trace expressions in a coordinate independent way.

The trajectory of the orbiting particle inside the storage ring on the Earth's surface is described by a worldline $t \mapsto \gamma_\omega(t)$ with coordinate components

$$\gamma_\omega{}^{\mathsf{a}}(t) = \begin{pmatrix} t \\ R \\ \Theta \\ \omega \sqrt{1 - \frac{r_S}{R}} \, t \bmod 2\pi \end{pmatrix}, \tag{2}$$

where for convenience the worldline is parameterized by the Killing time t and not with
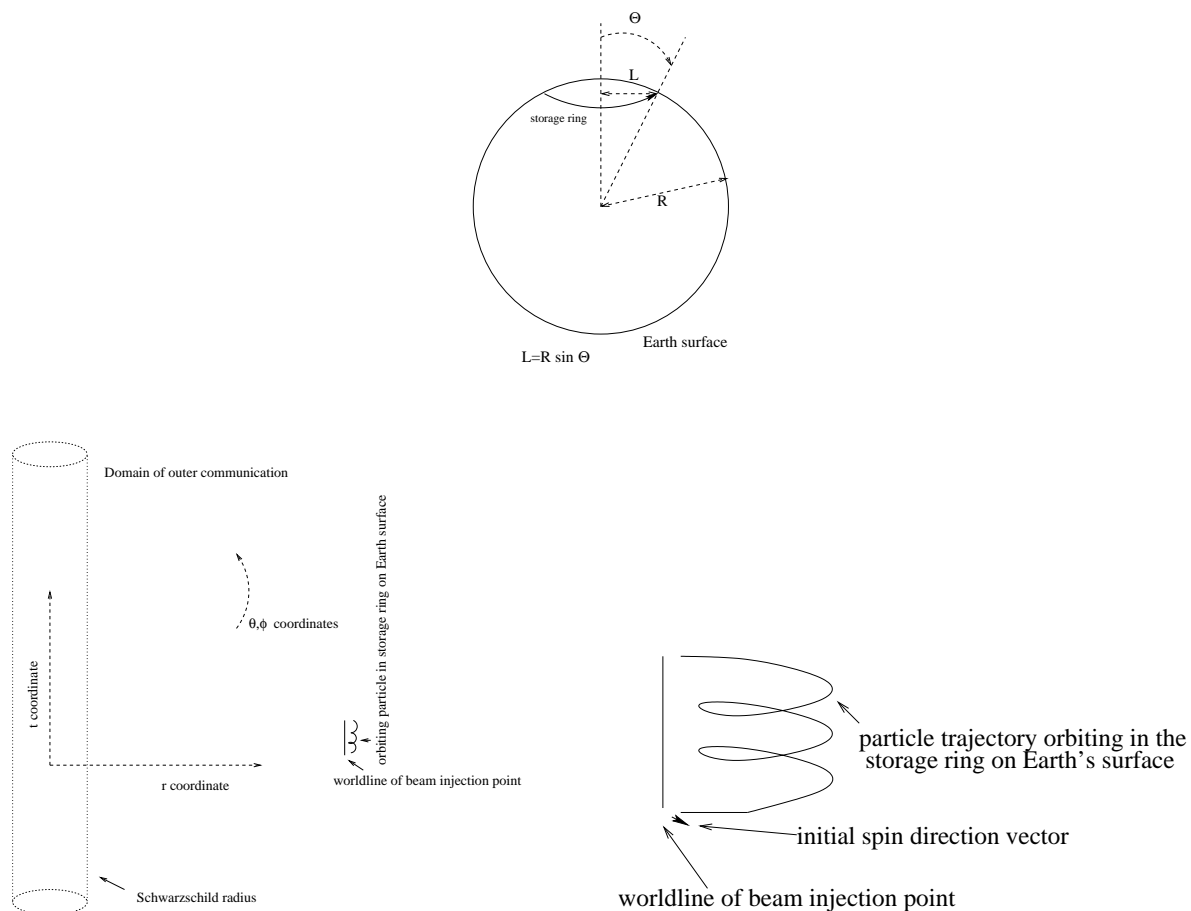
Figure 1. The outline of the kinematic setting of the experiment. Top panel: the particle storage ring is sitting on the Earth's surface. The radius of the Earth is denoted by R, the storage ring radius by L, and we set the North pole of our spherical coordinates by convention to the center of the storage ring. Bottom left panel: illustration of the laboratory setting in Earth's Schwarzschild spacetime. Throughout the paper the Schwarzschild coordinates t, r, ϑ, φ are used. Bottom right panel: a zoom of the particle's orbiting trajectory. The initial spin direction vector is Fermi-Walker transported along the worldline of the orbiting particle in Schwarzschild spacetime. The worldline of the beam injection point, i.e., the laboratory worldline is also shown, along which the initial spin vector can also be Fermi-Walker transported.

its proper time. Here, ω denotes the circular frequency of the orbiting particle trajectory, in terms of the proper time of the laboratory system. It is seen that the particles are assumed to be orbiting on a closed circular trajectory, i.e., a beam balanced against falling towards the Earth is assumed. This is justified by the fact that according to [7] an electrostatic beam focusing optics is used in the g-2 experimental setup, which is resting on the surface of the Earth, together with the storage ring. The initial spin direction vector at $t = 0$ is a unit pseudolength spacelike vector, orthogonal to the curve $t \mapsto \gamma_\omega(t)$. The amount of precession can be quantified via also evolving the initial spin direction vector along the worldline of the beam injection point of the storage ring

(laboratory observer), described by the curve $t \mapsto \gamma_0(t)$ having coordinate components

$$\gamma_0{}^{\mathsf{a}}(t) = \begin{pmatrix} t \\ R \\ \Theta \\ 0 \end{pmatrix}. \tag{3}$$

The worldlines $t \mapsto \gamma_\omega(t)$ and $t \mapsto \gamma_0(t)$ intersect at each full revolution, i.e., at each $t = n \frac{2\pi}{\omega\sqrt{1-\frac{r_S}{R}}}$, with n being any non-negative integer. In these intersection points the propagated spin direction vectors can be eventually compared. The unit tangent vector fields, i.e., the four velocity fields of these curves are $t \mapsto u_\omega{}^{\mathsf{a}}(t) := \frac{1}{\Lambda_\omega(t)} \dot{\gamma}_\omega{}^{\mathsf{a}}(t)$ and $t \mapsto u_0{}^{\mathsf{a}}(t) := \frac{1}{\Lambda_0(t)} \dot{\gamma}_0{}^{\mathsf{a}}(t)$, with $\Lambda_\omega := \sqrt{g_{\mathsf{ab}} \dot{\gamma}_\omega{}^{\mathsf{a}} \dot{\gamma}_\omega{}^{\mathsf{b}}}$ and $\Lambda_0 := \sqrt{g_{\mathsf{ab}} \dot{\gamma}_0{}^{\mathsf{a}} \dot{\gamma}_0{}^{\mathsf{b}}}$, respectively.

In order to evaluate the spin direction vector along any point of the worldline $t \mapsto \gamma_\omega(t)$ or $t \mapsto \gamma_0(t)$, it needs to be transported along the pertinent trajectories. This is described by the *Fermi-Walker transport*, i.e., by the *relativistic gyroscopic transport* [22]. Let u^d be a future directed unit timelike vector field, then the *Fermi-Walker derivative* of a vector field w^b along u^d is defined as:

$$D_u^F w^b := u^d \nabla_d w^b + g_{ac} w^a u^b u^d \nabla_d u^c - g_{ac} w^a u^c u^d \nabla_d u^b, \tag{4}$$

where ∇_d denotes the Levi-Civita covariant derivation associated to the metric g_{ab}. The Fermi-Walker derivative is distinguished by the fact that $D_u^F u^b = 0$ holds, as well as the property that for any two vector field w^b and v^b satisfying $D_u^F w^b = 0$ and $D_u^F v^b = 0$, the identity $u^a \nabla_a (g_{bc} w^b v^c) = 0$ holds. In particular, whenever one has $D_u^F w^b = 0$, then also $u^a \nabla_a (g_{bc} u^b w^c) = 0$ and $u^a \nabla_a (g_{bc} w^b w^c) = 0$ hold. A vector field w^b is said to be Fermi-Walker transported along the integral curves of a future directed timelike unit vector field u^d, whenever the equation

$$D_u^F w^b = 0 \tag{5}$$

is satisfied, which is just the relativistic gyroscope equation [15, 16]. The rationale behind considering the Fermi-Walker transport as a relativistic model of the gyroscope evolution is that for the transport of a vector field w^b along a timelike curve with future directed unit tangent vector field u^d, the initial constraints

$$\begin{aligned} g_{ab} u^a u^b &= 1, \\ g_{ab} w^a w^b &= -1, \\ g_{ab} u^a w^b &= 0 \end{aligned} \tag{6}$$

are conserved during evolution, and no artificial vorticity is added. Note, that physically the spin vector has constant pseudolength and is always perpendicular to the worldline of the particle, and this constraint needs to be preserved throughout the evolution. Also note, that intuitively the Fermi-Walker transport can be regarded as the parallel transport of a rigid orthonormal frame along a unit timelike vector field, the timelike element of the frame coinciding to that of the transporting vector field.

Whenever an electromagnetic field F_{ab} is also present, the charged particles with spin are governed by the equations of motion

$$u^a \nabla_a u^b = -\frac{q}{m} g^{bc} F_{cd} u^d,$$

$$D_u^F w^b = -\frac{\mu}{s} \left(g^{bc} F_{cd} - u^b u^c F_{cd} - g^{bc} F_{ce} u^e u^f g_{fd} \right) w^d, \tag{7}$$

where the first equation is the relativistic Newton equation with the electromagnetic force, and the second equation is the *Bargmann-Michel-Telegdi (BMT) equation* [24, 25]. Here, m denotes the particle mass, q denotes the particle charge, μ denotes the magnetic moment of the particle, and s denotes the spin magnitude ($s = \frac{1}{2}, 1, \frac{3}{2}, 2, \ldots$ for particles), while u^a is the four velocity of the particle and w^b is the spin direction vector of the particle.

Let us note that for charged spinning objects with non-trivial internal structure the BMT equation cannot directly be applied. Instead it can be regarded as a special limiting case of the so-called electromagnetically extended Mathisson-Papapetrou-Dixon (MPD) equations [26, 27, 28, 29, 30], which describe in the pole-dipole approximation the motion of a charged spinning body on a curved spacetime in the presence of electromagnetic field. When the electromagnetic dipole moment tensor is taken to be proportional to the spin tensor, and the curvature effects and the second order spin effects are all neglected, and after introducing a spin supplementary condition‡, the BMT equation is obtained. In the present context the treated objects are charged particles with spin without relevant internal structure, and therefore the BMT equation can be safely considered to be enough to describe the spin propagation, and is indeed used for the engineering design of accelerator facilities for spin-polarized particles.

In Sections 3, 4, 5 merely the Fermi-Walker transport $D_u^F w^b = 0$, i.e., the gyroscopic kinematics of the spin direction vector along the worldlines Eq.(2) and Eq.(3) will be studied in order to extract the Thomas precession over a Schwarzschild background. These results apply to any forced circular motion over a Schwarzschild background. Following that, in Sections 6, 7, 8, 9 the GR modifications to the electromagnetic (Larmor) precession is quantified, which contributes in addition when the forced circular orbit is achieved via an electromagnetic field acting on a charged particle.

3. The absolute Fermi-Walker transport of four vectors

The Fermi-Walker transport differential equation $D_{\frac{1}{\Lambda}\dot\gamma}^F w = 0$ of a vector field w along a curve $\lambda \mapsto \gamma(\lambda)$ reads in components as

$$D_{\frac{1}{\Lambda}\dot\gamma}^F w^b(\gamma(\lambda)) =$$
$$\frac{1}{\Lambda(\lambda)}\frac{\mathrm{d}}{\mathrm{d}\lambda}w^b(\gamma(\lambda)) + \frac{1}{\Lambda(\lambda)}\dot\gamma^d(\lambda)\,\Gamma_{dc}^b(\gamma(\lambda))\,w^c(\gamma(\lambda))$$
$$+ \frac{1}{\Lambda(\lambda)}g_{ac}(\gamma(\lambda))w^a(\gamma(\lambda))\frac{1}{\Lambda^2(\lambda)}\dot\gamma^b(\lambda)\frac{\mathrm{d}}{\mathrm{d}\lambda}\dot\gamma^c(\lambda)$$
$$+ \frac{1}{\Lambda(\lambda)}g_{ac}(\gamma(\lambda))w^a(\gamma(\lambda))\frac{1}{\Lambda^2(\lambda)}\dot\gamma^b(\lambda)\dot\gamma^d(\lambda)\Gamma_{de}^c(\gamma(\lambda))\dot\gamma^e(\lambda)$$
$$- \frac{1}{\Lambda(\lambda)}g_{ac}(\gamma(\lambda))w^a(\gamma(\lambda))\frac{1}{\Lambda^2(\lambda)}\dot\gamma^c(\lambda)\frac{\mathrm{d}}{\mathrm{d}\lambda}\dot\gamma^b(\lambda)$$

‡ It is necessary to introduce spin supplementary conditions (SSCs) as the MPD equations are not closed. One can use, e.g., the Mathisson-Pirani [26, 31] or the Tulczyjew-Dixon [28, 32] SSCs.

$$-\frac{1}{\Lambda(\lambda)}g_{\mathsf{ac}}(\gamma(\lambda))w^{\mathsf{a}}(\gamma(\lambda))\frac{1}{\Lambda^2(\lambda)}\dot{\gamma}^{\mathsf{c}}(\lambda)\dot{\gamma}^{\mathsf{d}}(\lambda)\Gamma^{\mathsf{b}}_{\mathsf{de}}(\gamma(\lambda))\dot{\gamma}^{\mathsf{e}}(\lambda)$$
$$= 0 \qquad (\lambda \in \mathbb{R}), \tag{8}$$

where $\Gamma^{\mathsf{a}}_{\mathsf{bc}}$ denotes the Christoffel symbols in the used coordinates, and

$$\lambda \mapsto \Lambda(\lambda) := \sqrt{g_{\mathsf{ab}}(\gamma(\lambda))\dot{\gamma}^{\mathsf{a}}(\lambda)\dot{\gamma}^{\mathsf{b}}(\lambda)} \tag{9}$$

is the pseudolength function of the tangent vector field $\lambda \mapsto \dot{\gamma}^{\mathsf{a}}(\lambda)$, and $\dot{()}$ denotes derivative against the curve parameter λ. In our calculations, for convenience reasons, we use the Killing time t as the parameter of the worldline curves.

In order to calculate Fermi-Walker transported vector fields $p \mapsto w_\omega{}^{\mathsf{a}}(p)$ and $p \mapsto w_0{}^{\mathsf{a}}(p)$ along the curves $t \mapsto \gamma_\omega(t)$ and $t \mapsto \gamma_0(t)$, we introduce the vector valued functions $\tilde{w}_\omega{}^{\mathsf{a}}(t) := (w_\omega{}^{\mathsf{a}} \circ \gamma_\omega)(t)$ and $\tilde{w}_0{}^{\mathsf{a}}(t) := (w_0{}^{\mathsf{a}} \circ \gamma_0)(t)$. One should note that the coordinate components of the tangent vectors

$$\dot{\gamma}_\omega{}^{\mathsf{a}}(t) = \begin{pmatrix} 1 \\ 0 \\ 0 \\ \omega\sqrt{1-\frac{r_S}{R}} \end{pmatrix}, \quad \dot{\gamma}_0{}^{\mathsf{a}}(t) = \begin{pmatrix} 1 \\ 0 \\ 0 \\ 0 \end{pmatrix} \tag{10}$$

of the curves Eq.(2) and Eq.(3) do not depend on Killing time, i.e., $\frac{\mathrm{d}}{\mathrm{d}t}\dot{\gamma}_\omega{}^{\mathsf{a}}(t) = 0$ and $\frac{\mathrm{d}}{\mathrm{d}t}\dot{\gamma}_0{}^{\mathsf{a}}(t) = 0$ hold. Using this, our Fermi-Walker transport equations $\Lambda_\omega \, D^F_{\frac{1}{\Lambda_\omega}\dot{\gamma}_\omega} w_\omega{}^{\mathsf{a}} = 0$ and $\Lambda_0 \, D^F_{\frac{1}{\Lambda_0}\dot{\gamma}_0} w_0{}^{\mathsf{a}} = 0$ simplify as

$$\frac{\mathrm{d}}{\mathrm{d}t}\tilde{w}_\omega{}^{\mathsf{b}}(t) \; + \; \dot{\gamma}_\omega{}^{\mathsf{d}}(t)\,\Gamma^{\mathsf{b}}_{\mathsf{dc}}(\gamma_\omega(t))\,\tilde{w}_\omega{}^{\mathsf{c}}(t)$$
$$+ \, g_{\mathsf{ac}}(\gamma_\omega(t))\tilde{w}_\omega{}^{\mathsf{a}}(t)\frac{1}{\Lambda^2(t)}\dot{\gamma}_\omega{}^{\mathsf{b}}(t)\dot{\gamma}_\omega{}^{\mathsf{d}}(t)\Gamma^{\mathsf{c}}_{\mathsf{de}}(\gamma_\omega(t))\dot{\gamma}_\omega{}^{\mathsf{e}}(t)$$
$$- \, g_{\mathsf{ac}}(\gamma_\omega(t))\tilde{w}_\omega{}^{\mathsf{a}}(t)\frac{1}{\Lambda^2(t)}\dot{\gamma}_\omega{}^{\mathsf{c}}(t)\dot{\gamma}_\omega{}^{\mathsf{d}}(t)\Gamma^{\mathsf{b}}_{\mathsf{de}}(\gamma_\omega(t))\dot{\gamma}_\omega{}^{\mathsf{e}}(t) = 0,$$
$$\frac{\mathrm{d}}{\mathrm{d}t}\tilde{w}_0{}^{\mathsf{b}}(t) \; + \; \dot{\gamma}_0{}^{\mathsf{d}}(t)\,\Gamma^{\mathsf{b}}_{\mathsf{dc}}(\gamma_0(t))\,\tilde{w}_0{}^{\mathsf{c}}(t)$$
$$+ \, g_{\mathsf{ac}}(\gamma_0(t))\tilde{w}_0{}^{\mathsf{a}}(t)\frac{1}{\Lambda^2(t)}\dot{\gamma}_0{}^{\mathsf{b}}(t)\dot{\gamma}_0{}^{\mathsf{d}}(t)\Gamma^{\mathsf{c}}_{\mathsf{de}}(\gamma_0(t))\dot{\gamma}_0{}^{\mathsf{e}}(t)$$
$$- \, g_{\mathsf{ac}}(\gamma_0(t))\tilde{w}_0{}^{\mathsf{a}}(t)\frac{1}{\Lambda^2(t)}\dot{\gamma}_0{}^{\mathsf{c}}(t)\dot{\gamma}_0{}^{\mathsf{d}}(t)\Gamma^{\mathsf{b}}_{\mathsf{de}}(\gamma_0(t))\dot{\gamma}_0{}^{\mathsf{e}}(t) \;\; = 0. \tag{11}$$

These linear differential equations need to be solved for the vector valued functions $t \mapsto \tilde{w}_\omega{}^{\mathsf{a}}(t)$ and $t \mapsto \tilde{w}_0{}^{\mathsf{a}}(t)$.

In order to solve the transport equations Eq.(11), one needs the expressions of the Christoffel symbols over Schwarzschild spacetime in our coordinate conventions. The only non-vanishing components at a point t, r, ϑ, φ are:

$$\Gamma^r_{tt}(t, r, \vartheta, \varphi) = \frac{(r - r_S)r_S}{2r^3},$$
$$\Gamma^t_{tr}(t, r, \vartheta, \varphi) = \frac{r_S}{2r(r - r_S)},$$
$$\Gamma^r_{rr}(t, r, \vartheta, \varphi) = -\frac{r_S}{2r(r - r_S)},$$

$$\Gamma^\vartheta_{r\vartheta}(t,r,\vartheta,\varphi) = \frac{1}{r},$$
$$\Gamma^\varphi_{r\varphi}(t,r,\vartheta,\varphi) = \frac{1}{r},$$
$$\Gamma^r_{\vartheta\vartheta}(t,r,\vartheta,\varphi) = -(r-r_S),$$
$$\Gamma^\varphi_{\vartheta\varphi}(t,r,\vartheta,\varphi) = \frac{\cos\vartheta}{\sin\vartheta},$$
$$\Gamma^r_{\varphi\varphi}(t,r,\vartheta,\varphi) = -(r-r_S)\sin^2\vartheta,$$
$$\Gamma^\vartheta_{\varphi\varphi}(t,r,\vartheta,\varphi) = -\sin\vartheta\cos\vartheta, \tag{12}$$

where the index symmetry property $\Gamma^a_{bc} = \Gamma^a_{cb}$ also needs to be taken into account. Observe, that due to the time translational and spherical symmetry of the Schwarzschild spacetime, the Christoffel symbols Γ^a_{bc} in our adapted coordinates only have ϑ dependence on $r = \mathrm{const}$ surfaces, i.e., also on the $r = R$ surface of the Earth. Since the curves $t \mapsto \gamma_\omega(t)$ and $t \mapsto \gamma_0(t)$ evolve on the Earth's surface, i.e., on the $r = R$ surface, the Christoffel symbol coefficients in Eq.(11) can merely have ϑ dependence along these curves. But since the pertinent curves are also $\vartheta = \mathrm{const}$, or more precisely $\vartheta = \Theta$ curves, the Christoffel symbol coefficients in Eq.(11) are completely constant along these. Similarly, the metric tensor components g_{ab} are also constants along these world lines. Moreover, also the vector valued functions $t \mapsto \dot{\gamma}_\omega{}^a(t)$ and $t \mapsto \dot{\gamma}_0{}^a(t)$ are constant. All these imply that the homogeneous linear differential equations Eq.(11) have constant coefficients, and therefore they can be eventually solved relatively easily, by a matrix exponentiation.

In the following, we denote by the symbol Γ^a_{bc} the particular constant value of the Schwarzschild Christoffel symbols along the curves $t \mapsto \gamma_\omega(t)$ or $t \mapsto \gamma_0(t)$, in our coordinates. Similarly, g_{ab} will denote the particular constant value of the metric tensor components along these world lines. These are obtained by simply substituting the values $r = R$, $\vartheta = \Theta$ and any value of φ and t into Eq.(12) and Eq.(1). Similarly, the symbol $\dot{\gamma}_\omega{}^a$ and $\dot{\gamma}_0{}^a$ will denote the constant value of the constant vector valued functions Eq.(10). Also, their pseudolengths are constant, $\Lambda_\omega = \sqrt{(1-\frac{r_S}{R})(1-\omega^2 R^2 \sin^2\Theta)}$ and $\Lambda_0 = \sqrt{1-\frac{r_S}{R}}$. With these notations, we are left with homogeneous linear differential equations with constant coefficients:

$$\frac{\mathrm{d}}{\mathrm{d}t}\tilde{w}_\omega{}^b(t) + \dot{\gamma}_\omega{}^d\,\Gamma^b_{dc}\,\tilde{w}_\omega{}^c(t)$$
$$+ g_{ca}\tilde{w}_\omega{}^c(t)\frac{1}{\Lambda_\omega{}^2}\dot{\gamma}_\omega{}^b\dot{\gamma}_\omega{}^d\Gamma^a_{de}\dot{\gamma}_\omega{}^e - g_{ca}\tilde{w}_\omega{}^c(t)\frac{1}{\Lambda_\omega{}^2}\dot{\gamma}_\omega{}^a\dot{\gamma}_\omega{}^d\Gamma^b_{de}\dot{\gamma}_\omega{}^e = 0,$$
$$\frac{\mathrm{d}}{\mathrm{d}t}\tilde{w}_0{}^b(t) + \dot{\gamma}_0{}^d\,\Gamma^b_{dc}\,\tilde{w}_0{}^c(t)$$
$$+ g_{ca}\tilde{w}_0{}^c(t)\frac{1}{\Lambda_0{}^2}\dot{\gamma}_0{}^b\dot{\gamma}_0{}^d\Gamma^a_{de}\dot{\gamma}_0{}^e - g_{ca}\tilde{w}_0{}^c(t)\frac{1}{\Lambda_0{}^2}\dot{\gamma}_0{}^a\dot{\gamma}_0{}^d\Gamma^b_{de}\dot{\gamma}_0{}^e = 0. \tag{13}$$

Direct evaluation shows that $\dot{\gamma}_0{}^d\,\Gamma^b_{dc} + g_{ca}\frac{1}{\Lambda_0{}^2}\dot{\gamma}_0{}^b\dot{\gamma}_0{}^d\Gamma^a_{de}\dot{\gamma}_0{}^e - g_{ca}\frac{1}{\Lambda_0{}^2}\dot{\gamma}_0{}^a\dot{\gamma}_0{}^d\Gamma^b_{de}\dot{\gamma}_0{}^e = 0$ holds, and thus any Fermi-Walker transported vector field $t \mapsto \tilde{v}_0{}^b(t)$ along the curve $t \mapsto \gamma_0(t)$ satisfies $\frac{\mathrm{d}}{\mathrm{d}t}\tilde{v}_0{}^b(t) = 0$ for all $t \in \mathbb{R}$. It also means that the Fermi-Walker derivative along $\frac{1}{\Lambda_0}\dot{\gamma}_0$ is proportional to the Lie derivative against the Killing time

translation vector field ∂_t. Taking this into account, our pair of differential equations simplify as

$$\frac{\mathrm{d}}{\mathrm{d}t}\tilde{w}_\omega{}^\mathsf{b}(t) = \mathcal{F}_\omega{}^\mathsf{b}{}_\mathsf{c}\,\tilde{w}_\omega{}^\mathsf{c}(t),$$
$$\frac{\mathrm{d}}{\mathrm{d}t}\tilde{w}_0{}^\mathsf{b}(t) = 0,\tag{14}$$

with

$$\mathcal{F}_\omega{}^\mathsf{b}{}_\mathsf{c} := -\dot{\gamma}_\omega{}^\mathsf{d}\,\Gamma^\mathsf{b}_{\mathsf{dc}} - g_{\mathsf{ca}}\frac{1}{\Lambda_\omega{}^2}\dot{\gamma}_\omega{}^\mathsf{b}\dot{\gamma}_\omega{}^\mathsf{d}\Gamma^\mathsf{a}_{\mathsf{de}}\dot{\gamma}_\omega{}^\mathsf{e} + g_{\mathsf{ca}}\frac{1}{\Lambda_\omega{}^2}\dot{\gamma}_\omega{}^\mathsf{a}\dot{\gamma}_\omega{}^\mathsf{d}\Gamma^\mathsf{b}_{\mathsf{de}}\dot{\gamma}_\omega{}^\mathsf{e}\tag{15}$$

being the *Fermi-Walker transport tensor*. The index pulled up version $\mathcal{F}_\omega{}^\mathsf{b}{}_\mathsf{c}g^{\mathsf{cd}}$ of the Fermi-Walker transport tensor can be shown to be antisymmetric by direct substitution. Therefore, it describes a Lorentz transformation generator. Moreover, $\mathcal{F}_\omega{}^\mathsf{b}{}_\mathsf{c}u_\omega{}^\mathsf{c} = 0$ holds by construction. Therefore, the Fermi-Walker transport tensor $\mathcal{F}_\omega{}^\mathsf{b}{}_\mathsf{c}$ describes a pure rotation in the space of $u_\omega{}^\mathsf{a}$-orthogonal vectors, called to be the *Thomas rotation*, and describes an absolute, i.e., observer independent rotation effect of the spin direction four vector. The concrete formula for the Fermi-Walker transport tensor is

$$\mathcal{F}_\omega{}^\mathsf{b}{}_\mathsf{c} = \frac{\omega\sqrt{1-\frac{r_S}{R}}}{1-\omega^2 L^2}$$
$$\begin{pmatrix} 0 & -\omega L\frac{L}{R}\frac{\left(1-\frac{3}{2}\frac{r_S}{R}\right)}{\left(1-\frac{r_S}{R}\right)^{\frac{3}{2}}} & -\omega LR\frac{\sqrt{1-\left(\frac{L}{R}\right)^2}}{\left(1-\frac{r_S}{R}\right)^{\frac{1}{2}}} & 0 \\ -\omega L\frac{L}{R}\left(1-\frac{3}{2}\frac{r_S}{R}\right)\left(1-\frac{r_S}{R}\right)^{\frac{1}{2}} & 0 & 0 & L\frac{L}{R}\left(1-\frac{3}{2}\frac{r_S}{R}\right) \\ -\omega L\frac{1}{R}\sqrt{1-\left(\frac{L}{R}\right)^2}\left(1-\frac{r_S}{R}\right)^{\frac{1}{2}} & 0 & 0 & \frac{L}{R}\sqrt{1-\left(\frac{L}{R}\right)^2} \\ 0 & -\frac{1}{R}\frac{\left(1-\frac{3}{2}\frac{r_S}{R}\right)}{\left(1-\frac{r_S}{R}\right)} & -\frac{R}{L}\sqrt{1-\left(\frac{L}{R}\right)^2} & 0 \end{pmatrix}$$

$$\tag{16}$$

in our coordinate conventions.

4. The relative Fermi-Walker transport as seen by the laboratory observer

As shown in the previous section, the Fermi-Walker transport of four vectors along $t \mapsto \gamma_\omega(t)$ is relatively simple notion described by the tensor $\mathcal{F}_\omega{}^\mathsf{b}{}_\mathsf{c}$. This needs to be translated to the transport of spatial vectors orthogonal to the laboratory observer $u_0{}^\mathsf{a}$, known to be the *Thomas precession*, which is a phenomenon also including effects relative to an observer. The procedure for quantifying this effect is rather well known already in the special relativistic scenario [33, 34].

Recall that the worldline of the beam injection point in the laboratory is the curve $t \mapsto \gamma_0(t)$ with a four velocity vector u_0, described by Eq.(3). Let us consider such a curve in each point of the storage ring. In other words: take the initial u_0 vector, and extend it via requiring $\mathcal{L}_{\partial_t}u_0 = 0$ to all t, defining the four velocity field of the curve $t \mapsto \gamma_0(t)$. It will obey the Fermi-Walker transport equation $D^F_{u_0}u_0 = \frac{1}{\Lambda_0}\mathcal{L}_{\partial_t}u_0 = 0$ along

itself. Then, extend it via the Lie transport $\mathcal{L}_{\partial_\varphi}$ to any point of the storage ring world sheet. This u_0 vector field will have a family of integral curves

$$t \mapsto \gamma_{0,\phi}(t) := \begin{pmatrix} t \\ R \\ \Theta \\ \phi \end{pmatrix} \tag{17}$$

indexed by $\phi \in [0, 2\pi[$. These will be the worldlines of the laboratory observer. Similarly, to Eq.(3), these will have the tangent vector field

$$\dot{\gamma}_0{}^{\mathsf{a}}(t, R, \Theta, \varphi) := \begin{pmatrix} 1 \\ 0 \\ 0 \\ 0 \end{pmatrix}, \tag{18}$$

and will have corresponding unit tangent vector field, i.e., four velocity $u_0{}^{\mathsf{a}}(t, R, \Theta, \varphi) := \frac{1}{\Lambda_0(t,R,\Theta,\varphi)}\dot{\gamma}_0{}^{\mathsf{a}}(t, R, \Theta, \varphi)$ with $\Lambda_0 := \sqrt{g_{\mathsf{ab}}\dot{\gamma}_0{}^{\mathsf{a}}\dot{\gamma}_0{}^{\mathsf{b}}} = \sqrt{1 - \frac{r_S}{R}}$. By this construction, the observer vector field u_0 is present at each point of the storage ring world sheet as shown in the top panel of Fig. 2, with the property $\mathcal{L}_{\partial_t}u_0 = 0$, $\mathcal{L}_{\partial_\varphi}u_0 = 0$. Actually, any vector v at the initial spacetime point can be spread as a reference vector to any point of the storage ring worldsheet, using this "Lie extension" $\mathcal{L}_{\partial_t}v = 0$, $\mathcal{L}_{\partial_\varphi}v = 0$. Since this spread vector field u_0 is vorticity-free, by means of Frobenius theorem it can be Einstein synchronized with orthogonal surfaces. These happen to coincide with the Killing time $t = \text{const}$ surfaces. The Einstein synchronized observer u_0 observes u_0-time evolution of vector fields along the curve $t \mapsto \gamma_\omega(t)$ via first spreading the initial vector using the above Lie extension as a reference, and then comparing the parallel transport evolution of the vector field along u_ω to the evolution of the Lie extended spread reference vector field along the u_0 parallel transport and subsequent ∂_φ Lie transport, in order to match the comparison spacetime point. This is illustrated in the bottom panel of Fig. 2. As a consequence, the covariant u_0-time derivative of vector fields v^a along $t \mapsto \gamma_\omega(t)$ formally can be written as $(v^a)' := \frac{\Lambda_\omega}{\Lambda_0}u_\omega{}^d\nabla_d v^a - u_0{}^d\nabla_d\check{v}^a - \omega\mathcal{L}_{\partial_\varphi}\check{v}^a$, where $\check{v}^a$ denotes the Lie extended vector field of the vector v^a at the given point of the curve, in order to make sense of the formula. In terms of coordinate components, this is described by

$$(v^{\mathsf{a}})'(\gamma_\omega(t)) =$$
$$\frac{\Lambda_\omega}{\Lambda_0}\left(\frac{1}{\Lambda_\omega}\frac{\mathrm{d}}{\mathrm{d}t}v^{\mathsf{a}}(\gamma_\omega(t)) + \frac{1}{\Lambda_\omega}\dot{\gamma}_\omega{}^{\mathsf{b}}\Gamma^{\mathsf{a}}_{\mathsf{bc}}v^{\mathsf{c}}(\gamma_\omega(t))\right) - \frac{1}{\Lambda_0}\dot{\gamma}_0{}^{\mathsf{b}}\Gamma^{\mathsf{a}}_{\mathsf{bc}}v^{\mathsf{c}}(\gamma_\omega(t)), \tag{19}$$

for a vector field $p \mapsto v^{\mathsf{a}}(p)$ along the curve $t \mapsto \gamma_\omega(t)$, in our coordinate choice.

It is important to recall that the evolving Fermi-Walker transported spin direction vector field w_ω is always orthogonal to u_ω. Let us denote by E_{u_ω} at a point of $t \mapsto \gamma_\omega(t)$ the subspace of u_ω-orthogonal vectors (u_ω-space vectors). Also, let E_{u_0} denote the orthogonal vectors to u_0 at a point of the laboratory observer world sheet.

Take a solution $w_\omega{}^a$ of the Fermi-Walker transport equation $D^F_{u_\omega}w_\omega{}^a = 0$, where the vector $w_\omega{}^a$ is initially (and thus also eternally) u_ω-space vector, i.e., resides in E_{u_ω}.
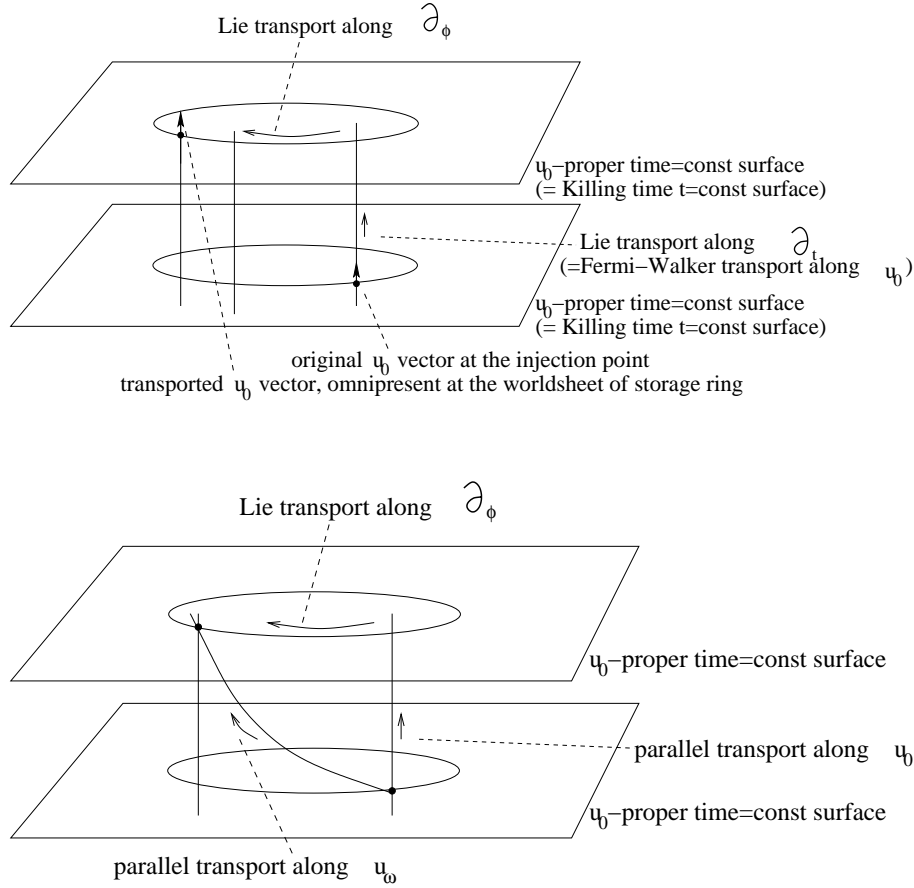
Figure 2. Top panel: illustration of how the four velocity vector u_0 of the beam injection point is spread along the worldsheet of the storage ring. It is spread via Lie extension, i.e., via requiring $\mathcal{L}_{\partial_t} u_0 = 0$ and $\mathcal{L}_{\partial_\varphi} u_0 = 0$, as described in the text. Since it is vorticity-free, by means of Frobenius theorem it can be Einstein synchronized by orthogonal surfaces, which happen to coincide with Killing time $t = $ const level surfaces. Actually, any vector at an initial point of the pertinent worldsheet can be extended to the entire worldsheet via such Lie extension. Bottom panel: illustration of how the Einstein synchronized observer u_0 measures evolution of vector fields along the curve $t \mapsto \gamma_\omega(t)$ in terms of observer time. The evolution of the vector field in terms of parallel transport of along u_ω is compared to the evolution of the Lie extended initial vector in terms of parallel transport along u_0 and subsequent Lie transport along ∂_φ in the matching comparison spacetime point.

The Einstein synchronized laboratory observer u_0, at a corresponding spacetime point, observes it via Lorentz boosting it back to E_{u_0}. That shall be denoted by w_{ω,u_0}, being an u_0-space vector at the same spacetime point. The Lorentz boost at a spacetime point from a future directed unit timelike vector u_1 to an other one u_2 is given by the formula:

$$B_{u_2,u_1}{}^b{}_c = \delta^b{}_c - \frac{(u_2{}^b + u_1{}^b)(u_2{}^d + u_1{}^d)g_{dc}}{1 + g_{ef}u_2{}^e u_1{}^f} + 2u_2{}^b g_{cd} u_1{}^d. \tag{20}$$

It is uniquely characterized by the following properties: it is the g_{ab}-isometry taking u_1 to u_2 (and thus E_{u_1} to E_{u_2}) that acts as the identity on the subspace $E_{u_1} \cap E_{u_2}$. With

this notation, one has that the original Fermi-Walker transported four vector field is described by $w_\omega{}^a = B_{u_\omega,u_0}{}^a{}_b w_{\omega,u_0}{}^b$. Since that was required to satisfy the Fermi-Walker transport equation, it must satisfy

$$u_\omega{}^d \nabla_d \left(B_{u_\omega,u_0}{}^a{}_b w_{\omega,u_0}{}^b \right) = -u_\omega{}^a (u_\omega{}^d \nabla_d u_\omega{}^c) g_{ce} (B_{u_\omega,u_0}{}^e{}_b w_{\omega,u_0}{}^b)$$
$$+ u_\omega{}^c (u_\omega{}^d \nabla_d u_\omega{}^a) g_{ce} (B_{u_\omega,u_0}{}^e{}_b w_{\omega,u_0}{}^b) \tag{21}$$

along the curve $t \mapsto \gamma_\omega(t)$. Applying now inverse boost B_{u_0,u_ω}, i.e., boost from u_ω to u_0, and using subsequently the Leibniz rule for covariant derivation, one infers that

$$u_\omega{}^d \nabla_d w_{\omega,u_0}{}^f = -u_\omega{}^d \left(B_{u_0,u_\omega}{}^f{}_a \nabla_d B_{u_\omega,u_0}{}^a{}_b \right) w_{\omega,u_0}{}^b$$
$$- B_{u_0,u_\omega}{}^f{}_a u_\omega{}^a (u_\omega{}^d \nabla_d u_\omega{}^c) g_{ce} B_{u_\omega,u_0}{}^e{}_b w_{\omega,u_0}{}^b$$
$$+ B_{u_0,u_\omega}{}^f{}_a u_\omega{}^c (u_\omega{}^d \nabla_d u_\omega{}^a) g_{ce} B_{u_\omega,u_0}{}^e{}_b w_{\omega,u_0}{}^b \tag{22}$$

must be satisfied. Using this and Eq.(19), the u_0-time derivative of the observed Fermi-Walker transported vector field w_{ω,u_0} can be given:

$$\left(w_{\omega,u_0}{}^f \right)' = \Phi^T_{\omega,u_0}{}^f{}_b \, w_{\omega,u_0}{}^b, \tag{23}$$

with the u_0-Fermi-Walker transport tensor

$$\Phi^T_{\omega,u_0}{}^f{}_b := -\frac{1}{\Lambda_0} \dot\gamma_0{}^d \Gamma^f_{db}$$
$$- \frac{1}{\Lambda_0} \dot\gamma_\omega{}^d \left(B_{u_0,u_\omega}{}^f{}_a \nabla_d B_{u_\omega,u_0}{}^a{}_b \right)$$
$$- \frac{1}{\Lambda_0} B_{u_0,u_\omega}{}^f{}_a \dot\gamma_\omega{}^a (u_\omega{}^d \nabla_d u_\omega{}^c) g_{ce} B_{u_\omega,u_0}{}^e{}_b$$
$$+ \frac{1}{\Lambda_0} B_{u_0,u_\omega}{}^f{}_a \dot\gamma_\omega{}^c (u_\omega{}^d \nabla_d u_\omega{}^a) g_{ce} B_{u_\omega,u_0}{}^e{}_b. \tag{24}$$

Using now the fact that we took special coordinates such that the coordinate components of $u_\omega{}^a$, $u_0{}^a$ and g_{ab} are constant, we get an explicit form for the coordinate components

$$\Phi^T_{\omega,u_0}{}^f{}_b = -\frac{1}{\Lambda_0} \dot\gamma_0{}^d \Gamma^f_{db} + \frac{1}{\Lambda_0} \dot\gamma_\omega{}^d \Gamma^f_{db} + \frac{1}{\Lambda_0} B_{u_0,u_\omega}{}^f{}_a \, \mathcal{F}_\omega{}^a{}_e \, B_{u_\omega,u_0}{}^e{}_b. \tag{25}$$

By direct substitution it is seen that the index pulled up version $\Phi^T_{\omega,u_0}{}^f{}_b g^{bc}$ is antisymmetric, and therefore corresponds to a Lorentz transformation generator. Also, it is seen that $\Phi^T_{\omega,u_0}{}^f{}_b u_0{}^b = 0$, and therefore it is an u_0-rotation generator, called to be the *Thomas precession*, which includes the relative observer effects as well. The concrete coordinate components of the Thomas precession tensor is

$$\Phi^T_{\omega,u_0}{}^a{}_b = \begin{pmatrix} 0 & 0 & 0 & 0 \\ 0 & 0 & 0 & \Phi^T_{\omega,u_0}{}^r{}_\varphi \\ 0 & 0 & 0 & \Phi^T_{\omega,u_0}{}^\vartheta{}_\varphi \\ 0 & \Phi^T_{\omega,u_0}{}^\varphi{}_r & \Phi^T_{\omega,u_0}{}^\varphi{}_\vartheta & 0 \end{pmatrix},$$

with

$$\Phi^T_{\omega,u_0}{}^\varphi{}_r = -\Phi^T_{\omega,u_0}{}^r{}_\varphi \frac{g^{\varphi\varphi}}{g^{rr}},$$

$$\Phi^T_{\omega,u_0}{}^\varphi{}_\vartheta = -\Phi^T_{\omega,u_0}{}^\vartheta{}_\varphi \frac{g^{\varphi\varphi}}{g^{\vartheta\vartheta}},$$

$$\Phi^T_{\omega,u_0}{}^r{}_\varphi = \omega L \frac{L}{R} \left((\gamma - 1) + \frac{r_S}{R} \left(1 - \frac{3}{2}\gamma \right) \right),$$

$$\Phi^T_{\omega,u_0}{}^{\vartheta}{}_{\varphi} = \omega(\gamma-1)\frac{L}{R}\sqrt{1-\left(\frac{L}{R}\right)^2}, \tag{26}$$

where the notation $\gamma := \frac{1}{\sqrt{1-\omega^2 L^2}}$ is used. It is remarkable that only the components $\Phi^T_{\omega,u_0}{}^r{}_{\varphi}$ and $\Phi^T_{\omega,u_0}{}^{\varphi}{}_r$ depend on r_S.

In order to extract the angular velocity vector of the u_0-rotation generator $\Phi^T_{\omega,u_0}{}^{\mathsf{f}}{}_{\mathsf{b}}$, one needs to take the spatial Hodge dual in the space of u_0. This is given by the formula

$$\Omega^T_{\omega,u_0}{}^{\mathsf{f}} := \frac{1}{2}\, u_0{}^{\mathsf{a}}\, \sqrt{-\det(g)}\epsilon_{\mathsf{abcd}}\, g^{\mathsf{bf}}\, \Phi^T_{\omega,u_0}{}^{\mathsf{c}}{}_{\mathsf{e}}\, g^{\mathsf{ed}}, \tag{27}$$

where $\det(g)$ denotes the determinant of the matrix of the metric g_{ab} in our coordinates, and ϵ_{abcd} is the Levi-Civita symbol. The concrete coordinate components of the Thomas precession angular velocity vector is

$$\Omega^T_{\omega,u_0}{}^{\mathsf{a}} = \begin{pmatrix} 0 \\ \omega(\gamma-1)\sqrt{1-\frac{r_S}{R}}\sqrt{1-\left(\frac{L}{R}\right)^2} \\ -\omega\frac{L}{R}\frac{1}{R}\frac{1}{\sqrt{1-\frac{r_S}{R}}}\left((\gamma-1)+\frac{r_S}{R}\left(1-\frac{3}{2}\gamma\right)\right) \\ 0 \end{pmatrix}. \tag{28}$$

Let us introduce the vector fields $\hat{r}^a := \frac{1}{\sqrt{g_{bc}(\partial_r)^b(\partial_r)^c}}(\partial_r)^a$, $\hat{\vartheta}^a := \frac{1}{\sqrt{g_{bc}(\partial_\vartheta)^b(\partial_\vartheta)^c}}(\partial_\vartheta)^a$, $\hat{\varphi}^a := \frac{1}{\sqrt{g_{bc}(\partial_\varphi)^b(\partial_\varphi)^c}}(\partial_\varphi)^a$, which are by construction an orthonormal basis in the space E_{u_0} at each point, in the direction of r, ϑ, φ. The metric projections of $\Omega^T_{\omega,u_0}{}^a$ onto this orthonormal basis is

$$-g_{ab}\,\hat{r}^a\,\Omega^T_{\omega,u_0}{}^b = \omega(\gamma-1)\sqrt{1-\left(\frac{L}{R}\right)^2},$$
$$-g_{ab}\,\hat{\vartheta}^a\,\Omega^T_{\omega,u_0}{}^b = -\omega\frac{L}{R}\frac{1}{\sqrt{1-\frac{r_S}{R}}}\left((\gamma-1)+\frac{r_S}{R}\left(1-\frac{3}{2}\gamma\right)\right),$$
$$-g_{ab}\,\hat{\varphi}^a\,\Omega^T_{\omega,u_0}{}^b = 0. \tag{29}$$

It is remarkable that only the ϑ projection carries all the r_S dependence.

The Thomas precession angular velocity magnitude is given by the length of the vector $\Omega^T_{\omega,u_0}{}^{\mathsf{a}}$, i.e., by

$$|\Omega|^T_{\omega,u_0} := \sqrt{-g_{\mathsf{ab}}\,\Omega^T_{\omega,u_0}{}^{\mathsf{a}}\,\Omega^T_{\omega,u_0}{}^{\mathsf{b}}}, \tag{30}$$

which can be evaluated to be

$$|\Omega|^T_{\omega,u_0} =$$

$$|\omega|\frac{1}{\sqrt{1-\frac{r_S}{R}}}\left((\gamma-1)^2\right.$$
$$+\left(\frac{r_S}{R}\right)\left(-\gamma^2\left(1+2\left(\frac{L}{R}\right)^2\right)+\gamma\left(2+3\left(\frac{L}{R}\right)^2\right)-\left(1+\left(\frac{L}{R}\right)^2\right)\right)$$
$$+\left.\left(\frac{r_S}{R}\right)^2\left(\frac{L}{R}\right)^2\left(\frac{3}{2}\gamma-1\right)^2\right)^{\frac{1}{2}}. \tag{31}$$

In the real experimental situation [4, 7] of g-2 experiments, the used observables are rather related to the oscillation frequency of various projections of the spin direction vector $w_{\omega,u_0}{}^a$, and not directly related to the magnitude of the precession angular velocity. Let d^a be a vector field defined along the orbiting curve $t \mapsto \gamma_\omega(t)$ with the property that its coordinate components $d^a(\gamma_\omega(t))$ are constant as a function of t in our adapted coordinates. We call such a vector field a corotating vector. Due to the definition of the covariant u_0-time derivative $(\cdot)'$, it shall obey the equation of motion

$$\left(d^a\right)' = \Phi^C_{\omega,u_0}{}^a{}_b\, d^b \tag{32}$$

with the definition $\Phi^C_{\omega,u_0}{}^a{}_b := \frac{1}{\Lambda_0}\left(\dot{\gamma}_\omega{}^c - \dot{\gamma}_0{}^c\right)\Gamma^a_{cb}$. That is due to Eq.(19) and to $\frac{d}{dt}\, d^a(\gamma_\omega(t)) = 0$. By construction or by direct substitution it is seen that the index pulled up version $\Phi^C_{\omega,u_0}{}^a{}_b\, g^{bc}$ is antisymmetric, and therefore $\Phi^C_{\omega,u_0}{}^a{}_b$ corresponds to a Lorentz transformation generator. Moreover $\Phi^C_{\omega,u_0}{}^a{}_b\, u_0{}^b = 0$ holds, and therefore, it corresponds to an u_0-rotation. The equation of motion Eq.(32) is therefore called the *cyclic motion*. The coordinate components of the cyclic motion tensor are:

$$\Phi^C_{\omega,u_0}{}^a{}_b = \begin{pmatrix} 0 & 0 & 0 & 0 \\ 0 & 0 & 0 & \Phi^C_{\omega,u_0}{}^r{}_\varphi \\ 0 & 0 & 0 & \Phi^C_{\omega,u_0}{}^\vartheta{}_\varphi \\ 0 & \Phi^C_{\omega,u_0}{}^\varphi{}_r & \Phi^C_{\omega,u_0}{}^\varphi{}_\vartheta & 0 \end{pmatrix},$$

with

$$\Phi^C_{\omega,u_0}{}^\varphi{}_r = -\Phi^C_{\omega,u_0}{}^r{}_\varphi \frac{g^{\varphi\varphi}}{g^{rr}},$$

$$\Phi^C_{\omega,u_0}{}^\varphi{}_\vartheta = -\Phi^C_{\omega,u_0}{}^\vartheta{}_\varphi \frac{g^{\varphi\varphi}}{g^{\vartheta\vartheta}},$$

$$\Phi^C_{\omega,u_0}{}^r{}_\varphi = -\omega R\left(1 - \frac{r_S}{R}\right)\left(\frac{L}{R}\right)^2,$$

$$\Phi^C_{\omega,u_0}{}^\vartheta{}_\varphi = -\omega\left(\frac{L}{R}\right)\sqrt{1 - \left(\frac{L}{R}\right)^2}. \tag{33}$$

This rotation generator tensor can be transformed to a more convenient form via an u_0 Hodge dualization

$$\Omega^C_{\omega,u_0}{}^f := \frac{1}{2}\, u_0{}^a\, \sqrt{-\det(g)}\,\epsilon_{abcd}\, g^{bf}\, \Phi^C_{\omega,u_0}{}^c{}_e\, g^{ed} \tag{34}$$

which defines the angular velocity vector of the cyclic motion. The coordinate components of the cyclic angular velocity vector is

$$\Omega^C_{\omega,u_0}{}^a = \begin{pmatrix} 0 \\ -\omega\sqrt{1 - \frac{r_S}{R}}\sqrt{1 - \left(\frac{L}{R}\right)^2} \\ \omega\frac{L}{R}\frac{1}{R}\sqrt{1 - \frac{r_S}{R}} \\ 0 \end{pmatrix}. \tag{35}$$

The observables in the real g-2 experiments are related to the oscillation frequency of projections of the spin direction vector $w_{\omega,u_0}{}^a$ onto corotating vectors, such as onto $\hat{\varphi}^a$.

It is seen that

$$\left(-g_{ab}\, d^a\, w_{\omega,u_0}{}^b\right)' = -\, g_{ab}\, \left(\Phi^T_{\omega,u_0} - \Phi^C_{\omega,u_0}\right)^b{}_c\, d^a\, w_{\omega,u_0}{}^c \tag{36}$$

holds, where the Leibniz rule, Eq.(23), Eq.(32), and the antisymmetry of $\Phi^C_{\omega,u_0}{}^c{}_d\, g^{de}$ has to be used. With a subsequent time derivation, one arrives at

$$\left(-g_{ab}\, d^a\, w_{\omega,u_0}{}^b\right)'' = -\, g_{ab}\, \left(\Phi^T_{\omega,u_0} - \Phi^C_{\omega,u_0}\right)^b{}_c\, \left(\Phi^T_{\omega,u_0} - \Phi^C_{\omega,u_0}\right)^c{}_d\, d^a\, w_{\omega,u_0}{}^d \tag{37}$$

where identity $\left(\Phi^T_{\omega,u_0} - \Phi^C_{\omega,u_0}\right)^a{}_b{}' = \Phi^C_{\omega,u_0}{}^a{}_c\left(\Phi^T_{\omega,u_0} - \Phi^C_{\omega,u_0}\right)^c{}_b - \left(\Phi^T_{\omega,u_0} - \Phi^C_{\omega,u_0}\right)^a{}_c\, \Phi^C_{\omega,u_0}{}^c{}_b$ has to be used in addition. From now on, the corotating vector d^a shall be assumed to be a unit vector, residing in E_{u_0}, and denote by $P_{(d)}{}^a{}_b := -d^a g_{cb} d^c$ the orthogonal projection operator onto d^a. Since $d^a = P_{(d)}{}^a{}_e\, d^e$ holds, moreover since $g_{ab}\, P_{(d)}{}^a{}_e = g_{ef}\, P_{(d)}{}^f{}_b$ holds, one obtains the identity

$$\left(-g_{ab}\, d^a\, w_{\omega,u_0}{}^b\right)'' = A_{ed}\, d^e\, w_{\omega,u_0}{}^d$$
with
$$A_{ed} := -g_{ef}\, \left(P_{(d)}{}^f{}_b\, \left(\Phi^T_{\omega,u_0} - \Phi^C_{\omega,u_0}\right)^b{}_c\, \left(\Phi^T_{\omega,u_0} - \Phi^C_{\omega,u_0}\right)^c{}_d\right). \tag{38}$$

Using now the fact that the tensor $\left(\Phi^T_{\omega,u_0} - \Phi^C_{\omega,u_0}\right)^b{}_c\, g^{cd}$ can be regarded as the u_0 Hodge dual of the vector $\left(\Omega^T_{\omega,u_0} - \Omega^C_{\omega,u_0}\right)^a$, the identity

$$A_{ed} =$$
$$-\, g_{ef}\, \Big(-\left|\Omega^T_{\omega,u_0} - \Omega^C_{\omega,u_0}\right|^2\, P_{(d)}{}^f{}_d$$
$$-\, P_{(d)}{}^f{}_b\, \left(\Omega^T_{\omega,u_0} - \Omega^C_{\omega,u_0}\right)^b\, \left(\Omega^T_{\omega,u_0} - \Omega^C_{\omega,u_0}\right)^c\, g_{cd}\Big) \tag{39}$$

follows. From Eq.(38) and Eq.(39) it follows that the projection $-g_{ab}\, d^a\, w_{\omega,u_0}{}^b$ has zero oscillation frequency whenever d^a points in the direction of the vector $\left(\Omega^T_{\omega,u_0} - \Omega^C_{\omega,u_0}\right)^a$. Moreover, it has oscillation frequency $\left|\Omega^T_{\omega,u_0} - \Omega^C_{\omega,u_0}\right|$ whenever d^a points in the direction $\hat{\varphi}^a$ (longitudinal direction), being orthogonal to $\left(\Omega^T_{\omega,u_0} - \Omega^C_{\omega,u_0}\right)^a$. Whenever d^a is orthogonal to both (transverse direction), the corresponding projection also oscillates with $\left|\Omega^T_{\omega,u_0} - \Omega^C_{\omega,u_0}\right|$. The experimental observables in the g-2 experiments are related to the oscillation frequency of the longitudinal direction, which evaluates as

$$\left|\Omega^T_{\omega,u_0} - \Omega^C_{\omega,u_0}\right| = |\omega|\, \gamma\, \sqrt{1 - 2\frac{r_S}{R}\left(\frac{L}{R}\right)^2 \frac{1 - \frac{9}{8}\frac{r_S}{R}}{1 - \frac{r_S}{R}}}. \tag{40}$$

It is interesting to note that from the metric projections of the vector $\left(\Omega^T_{\omega,u_0} - \Omega^C_{\omega,u_0}\right)^a$, only the ϑ projection has dependence on r_S:

$$-g_{ab}\, \hat{r}^a\, (\Omega^T_{\omega,u_0} - \Omega^C_{\omega,u_0})^b = \omega\gamma\sqrt{1 - \left(\frac{L}{R}\right)^2},$$
$$-g_{ab}\, \hat{\vartheta}^a\, (\Omega^T_{\omega,u_0} - \Omega^C_{\omega,u_0})^b = -\omega\gamma\frac{L}{R}\left(1 - \frac{3}{2}\frac{r_S}{R}\right)\frac{1}{\sqrt{1 - \frac{r_S}{R}}},$$
$$-g_{ab}\, \hat{\varphi}^a\, (\Omega^T_{\omega,u_0} - \Omega^C_{\omega,u_0})^b = 0. \tag{41}$$

All these expressions were derived and cross-checked using the GRTensorII Maple package [35]. The above calculations will also be made available as supplementary material.

5. Evaluation of the GR correction for Thomas precession

As shown in the previous section, the expression for the precession angular velocity $|\Omega|^T_{\omega,u_0}$ can be obtained as an analytical formula Eq.(31). Its Minkowski limit is

$$\left.|\Omega|^T_{\omega,u_0}\right|_{r_S=0} = |\omega|\,(\gamma-1) = |\omega|\frac{\beta^2\gamma^2}{1+\gamma}, \tag{42}$$

with the notation $\beta := \omega\,L$. This is the special relativistic formula for Thomas precession, presented also in many textbooks [33, 34]. The first order correction of GR can be obtained via taking the first Taylor term of $|\Omega|^T_{\omega,u_0}$ as a function of r_S. The first order absolute error turns out to be:

$$r_S\left(\left.\frac{\mathrm{d}}{\mathrm{d}r_S}|\Omega|^T_{\omega,u_0}\right|_{r_S=0}\right) = -\frac{r_S}{2R}\frac{L^2}{R^2}|\omega|\frac{2\gamma^2+\gamma-1}{1+\gamma}. \tag{43}$$

The quotient of Eq.(43) and Eq.(42) gives the relative systematic error of $|\Omega|^T_{\omega,u_0}$ due to neglection of GR, which evaluates to

$$-\frac{r_S}{2R}\frac{L^2}{R^2}\frac{2\gamma^2+\gamma-1}{\beta^2\gamma^2}. \tag{44}$$

It is seen that in the ultrarelativistic limit ($|\beta|\to 1$), it evaluates to $-\frac{r_S}{R}\frac{L^2}{R^2}$, whereas in the nonrelativistic limit ($|\beta|\to 0$) it can be approximated as $-\frac{r_S}{R}\frac{L^2}{R^2}\frac{1}{\beta^2}$. It is quite remarkable that the relative systematic error at the nonrelativistic limit diverges as $\frac{1}{\beta^2}$, which can be understood by recalling that the small special relativistic phenomenon of Thomas precession is competing against the small GR correction in that regime, and the GR correction happens to win in that limit. An other feature of the GR correction is that the vector $\Omega^T_{\omega,u_0}{}^a$ tilts with respect to the Minkowski limit. To the first order, the tilt angle can be estimated from the first Taylor term of Eq.(29) in terms of r_S and from Eq.(42), and is seen to be:

$$\frac{r_S}{R}\frac{L}{R}\frac{\left(\gamma-\frac{1}{2}\right)(\gamma+1)}{\beta^2\gamma^2}. \tag{45}$$

It is seen that in the ultrarelativistic limit the tilt angle becomes $\frac{r_S}{R}\frac{L}{R}$, whereas in the nonrelativistic limit it becomes $\frac{r_S}{R}\frac{L}{R}\frac{1}{\beta^2}$. When the oscillation frequency Eq.(40) of the longitudinal or transverse spin projection is considered, it behaves as

$$\left.\left|\Omega^T_{\omega,u_0}-\Omega^C_{\omega,u_0}\right|\right|_{r_S=0} = |\omega|\,\gamma \tag{46}$$

in the Minkowski limit, and its first order correction is

$$r_S\left(\left.\frac{\mathrm{d}}{\mathrm{d}r_S}\left|\Omega^T_{\omega,u_0}-\Omega^C_{\omega,u_0}\right|\right|_{r_S=0}\right) = -\frac{r_S}{R}\left(\frac{L}{R}\right)^2|\omega|\gamma, \tag{47}$$

and therefore its relative systematic error is $-\frac{r_S}{R}\left(\frac{L}{R}\right)^2$, independent of the velocity $|\beta|$. The vector $\left(\Omega^T_{\omega,u_0}-\Omega^C_{\omega,u_0}\right)^a$ also suffers a tilt, and the tilt angle is seen to be

$$-\frac{r_S}{R}\frac{L}{R} \tag{48}$$

from Eq.(46) and from Eq.(41), independently of the velocity $|\beta|$.

In the real muon g-2 experiment, the muons are injected with a relativistic Lorentz dilatation factor $\gamma \approx 29.3$ to the storage ring [4, 7]. This means a velocity relative to the speed of light $|\beta| \approx 0.999417412329374$, i.e., the muons are ultrarelativistic and one is in the $|\beta| \to 1$ limit. Therefore, the Thomas precession frequency as well as the longitudinal spin oscillation frequency is modified by a relative systematic error of

$$-\frac{r_S}{R}\frac{L^2}{R^2} \tag{49}$$

in the muon g-2 experiment. Using now Eq.(49) and the radius and Schwarzschild radius of the Earth, $R \approx 6.371 \cdot 10^6$ m and $r_S \approx 9 \cdot 10^{-3}$ m, and the storage ring radius $L \approx 7.5$ m, one infers that the relative systematic error made when neglecting GR in the estimation of Thomas precession frequency is

$$\approx -2 \cdot 10^{-21}, \tag{50}$$

which is negligible, given the present experimental accuracy. The most sensitive observable to the GR correction seems to be the tilt of the spin precession plane against the nominal horizontal plane, which is $\approx 1.7 \cdot 10^{-15} \frac{1}{\beta^2}$ radians with the parameters of the existing g-2 magnet setup. It is seen that an experimental detection of GR effects are only possible with sufficiently low $|\beta|$ and sufficiently large angular resolution, which is not realistic e.g. in a muon g-2 experiment. Moreover in the above corrections the effects of GR on the electrodynamics of the beam optics is not yet accounted for, which we quantify in the coming sections.

6. Electromagnetic fields in an idealized storage ring over Schwarzschild

In this section, the electromagnetic fields in an idealized storage ring [7] over a Schwarzschild background spacetime is outlined, which guides the particle beam along the nominal beam trajectory Eq.(2).

The most important electromagnetic field in a storage ring is usually, a homogeneous magnetic field, which forces the particles onto a closed circular orbit at the nominal trajectory. The first task is to define such a field configuration over our Schwarzschild background. In order to do that, recall that the outward pointing unit normal vector field of the surface $r = $ const surface is called the radial unit vector field, and is denoted by $\hat{r}^a$. Its components in our coordinate conventions are

$$\hat{r}^{\mathsf{a}}(t, r, \vartheta, \varphi) = \begin{pmatrix} 0 \\ \sqrt{1 - \frac{r_S}{r}} \\ 0 \\ 0 \end{pmatrix}. \tag{51}$$

The intersection of an $r = $ const surface with a Killing time $t = $ const surface is a two-sphere. The induced metric $g_{ab} + \hat{r}_a\hat{r}_b$ on it is just the round two-sphere metric with radius r. Besides the induced metric, on the pertinent surface the embedded flat metric can also be defined by $g_{ab} + \hat{r}_a\hat{r}_b - \mathrm{d}r_a\mathrm{d}r_b$, where $\mathrm{d}r$ denotes the exterior derivative of

the radius function r. This surface has a vector field on it defined by taking the radial unit vector field at a preferred point, and parallel transporting it to any point of the two-sphere along a geodesic, in terms of the embedded flat metric. That vector field, when initialized from the storage ring axis, i.e., from $\vartheta = 0$, is denoted by $\hat{v}^a$, and is called the vertical unit vector field. Its components in our coordinate conventions are

$$\hat{v}^{\sf a}(t, r, \vartheta, \varphi) = \begin{pmatrix} 0 \\ \cos\vartheta \\ -\frac{1}{r}\sin\vartheta \\ 0 \end{pmatrix}. \tag{52}$$

Note that the unit length and the parallel transport is understood in the embedded flat metric on the surface, and not in the merely restricted Schwarzschild metric to the surface. These vector fields and their geometric construction is illustrated in Fig. 3.
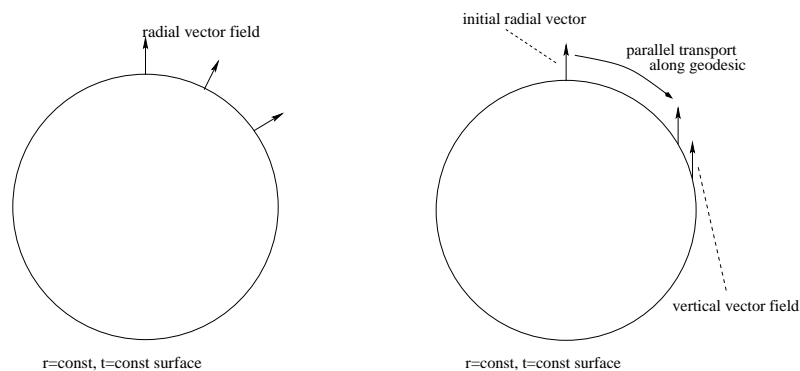
Figure 3. Left panel: illustration of the outward pointing radial unit vector field $\hat{r}^a$ on an $r = \mathrm{const}$, $t = \mathrm{const}$ surface. Right panel: illustration of the geometric construction of the vertical unit vector field $\hat{v}^a$ on an $r = \mathrm{const}$, $t = \mathrm{const}$ surface. The outward pointing radial unit vector field is taken at a preferred point, and it is parallel transported along geodesics to other points of the surface, in terms of the embedded flat metric.

The static, axisymmetric, homogeneous vertical magnetic vector field B^a, which forces the particles on a cyclotronic motion in the storage ring, is simply defined by a radial scalar multiple of the vertical unit vector field $\hat{v}^a$. Namely, one has the ansatz $B^a(t, r, \vartheta, \varphi) = b(r)\,\hat{v}^a(t, r, \vartheta, \varphi)$ with $r \mapsto b(r)$ being a radial function such that the electromagnetic field corresponding to B^a satisfies the vacuum Maxwell equations [36]. This implies that in our coordinates it has the components

$$B^{\sf a}(t, r, \vartheta, \varphi) = B\,\sqrt{\frac{1 - \frac{r_S}{r}}{1 - \frac{r_S}{R}\left(\frac{L}{R}\right)^2}}\begin{pmatrix} 0 \\ \cos\vartheta \\ -\frac{1}{r}\sin\vartheta \\ 0 \end{pmatrix}, \tag{53}$$

with B being a constant. It is normalized such that on the $r = R$ and $\vartheta = \Theta$ surface, it has pseudolength equal to the constant $|B|$. The magnetic component of

our electromagnetic field is defined by the Hodge dual of B^{a} in the laboratory frame u_0:

$$F_{\mathsf{bc}}^{B} := -u_0{}^{\mathsf{a}}\sqrt{-\det(g)}\epsilon_{\mathsf{abcd}}B^{\mathsf{d}}. \tag{54}$$

Direct substitution shows that F_{bc}^{B} satisfies the vacuum Maxwell equations over Schwarzschild spacetime.

In the muon g-2 or EDM experimental settings [7], an electrostatic beam focusing optics is used to maintain the beam stability. Since this beam optics is standing on the Earth's surface together with the storage ring, on the average it exerts a radial electrostatic field at the nominal trajectory, balancing the beam against falling towards the Earth. This electrostatic field, being radial, has the form $E_R{}^a(t, r, \vartheta, \varphi) = e(r)\,\hat{r}^a(t, r, \vartheta, \varphi)$, where the radial function $r \mapsto e(r)$ has to be chosen such that the electromagnetic field corresponding to $E_R{}^a$ satisfies the vacuum Maxwell equations. This implies that in our coordinates it has components

$$E_R{}^{\mathsf{a}}(t, r, \vartheta, \varphi) = E_R\,\frac{R^2}{r^2}\begin{pmatrix} 0 \\ \sqrt{1-\frac{r_S}{r}} \\ 0 \\ 0 \end{pmatrix}, \tag{55}$$

with E_R being a constant. It is normalized such that on the $r = R$ surface, it has pseudolength equal to the constant $|E_R|$. The electric component of our electromagnetic field is defined by $E_R{}^{\mathsf{a}}$ and u_0:

$$F_{ab}^{E_R} := u_0{}^c g_{ca} E_R{}^d g_{db} - u_0{}^c g_{cb} E_R{}^d g_{da}. \tag{56}$$

Direct substitution shows that $F_{ab}^{E_R}$ satisfies the vacuum Maxwell equations over Schwarzschild spacetime.

In the EDM experimental settings [7], sometimes a mixed electrostatic-magnetostatic storage ring is used, or a pure electrostatic storage ring. These employ an outward pointing cylindrical electrostatic field, being the electric field of a uniformly charged infinite wire in an idealized model. The field of such a wire could be directly calculated, since the Green's function of electrostatics/magnetostatics is well understood over a Schwarzschild background [37]. The evaluation of the pertinent Green's integral over the wire, however, becomes quite complicated if one would like an analytical formula. Therefore, it is easier to construct the pertinent field configuration using symmetry ansatzes. As it is well-known, in the Minkowski limit, the field of such a uniformly charged wire, comoving with the observer u_0, and placed at $\vartheta = 0$ and $\vartheta = \pi$ is known to be a cylindric one, with field strength decaying like $\sim\frac{1}{r \sin\vartheta}$, and its electrostatic potential being of the form $\sim \ln(r \sin\vartheta) + \text{const}$. Our ansatz over the Schwarzschild background therefore shall be that the electromagnetic vector potential has the form

$$A_{\mathsf{a}}(t, r, \vartheta, \varphi) = \left(\ f(r)\,\ln(\sin\vartheta) + g(r),\ \ 0,\ \ 0,\ \ 0\ \right) \tag{57}$$

which should solve the vacuum Maxwell equations for $r > r_S$, outside the wire singularity $\vartheta = 0$ and $\vartheta = \pi$. That requirement determines the unknown radial functions $f(r)$ and

$g(r)$ up to four integration constants a, b, c, d, and one arrives at the solution

$$A_t(t, r, \vartheta, \varphi) = a \left(\ln(\sin \vartheta) + \left(1 - \frac{r_S}{r} \right) \ln(r - r_S) \right)$$
$$+ b \left(\frac{1}{r} \ln(\sin \vartheta) - \frac{1}{r_S} \ln(r) + \frac{1}{r_S} \left(1 - \frac{r_S}{r} \right) \ln(r - r_S) \right)$$
$$- c \frac{1}{r} + d. \tag{58}$$

Since the field strength tensor is the exterior derivative of A_a, it is invariant to the choice of the integration constant d, and thus one may set $d = 0$ by convention. Also, the Maxwell's equations are linear, and thus the shape of the field configuration is invariant to the normalization of the solution, and therefore, e.g., one may set $a = 1$ by convention, in order to determine the shape of the field. Given these choices, the total charge within an $r = \text{const}$ sphere of a solution Eq.(58) evaluates as $\int_{S^2_{(r=\text{const})}} (*\mathrm{d}A) = 2\pi \left(2 \left(-r - (b + r_S) \right) \ln(r - r_S) - c \right) + b \, 2 \, (\ln(2) - 1))$. If one requires that the charge under the $r = \text{const}$ two-spheres should not diverge as $r \to r_S$, the equality $b = -r_S$ follows. With this condition, the charge under an $r = \text{const}$ two-sphere shall be $2\pi \left(2 \left(-r - c \right) - r_S \, 2 \, (\ln(2) - 1) \right)$, meaning that the charge density in terms of r along the wire is uniform, as illustrated in Fig. 4. The last integration constant c can be fixed by requiring that the charge under the sphere $r = r_S$ must vanish, and then $c = -r_S \ln(2)$ follows. Thus, the field strength tensor $F^{E_H}_{ab}$ of a uniformly charged vertical wire suspended over a Schwarzschild background becomes a constant factor times $\mathrm{d}A$, with A taken from Eq.(58) and $a = 1$, $b = -r_S$, $c = -r_S \ln(2)$, $d = 0$. If one wishes to express that in terms of an electric vector field $E_H{}^a$ in the space of the observer u_0, defined in terms of $F^{E_H}_{ab} = u_0{}^c g_{ca} E_H{}^d g_{db} - u_0{}^c g_{cb} E_H{}^d g_{da}$, then one arrives at the expression

$$E_H{}^{\mathsf{a}}(t, r, \vartheta, \varphi) = E_H \frac{L}{r \sin \vartheta} \sqrt{1 - \frac{r_S}{r}} \mathcal{N}_{r_S} \begin{pmatrix} 0 \\ \sin \vartheta \left(1 + \frac{r_S}{r} \ln(\frac{1}{2} \sin \vartheta) \right) \\ \frac{1}{r} \cos \vartheta \\ 0 \end{pmatrix},$$

$$\text{with } \mathcal{N}_{r_S} := \left(\left(\frac{L}{R} \right)^2 \left(1 + \frac{r_S}{R} \ln \left(\frac{L}{2R} \right) \right)^2 + \left(1 - \left(\frac{L}{R} \right)^2 \right) \left(1 - \frac{r_S}{R} \right) \right)^{-\frac{1}{2}} \tag{59}$$

where the normalization factor E_H is a real constant. The symbol $\mathcal{N}_{r_S}$ was introduced for brevity. The formula is normalized such that at the $r = R$, $\vartheta = \Theta$ location of the nominal beam line, the vector field $E_H{}^a$ has pseudolength equal to the constant $|E_H|$. As a cross-check, direct evaluation also shows that the field strength tensor $F^{E_H}_{ab} = u_0{}^c g_{ca} E_H{}^d g_{db} - u_0{}^c g_{cb} E_H{}^d g_{da}$ indeed satisfies the vacuum Maxwell equations over Schwarzschild spacetime.

The total electromagnetic field strength tensor is then $F_{ab} := F^B_{ab} + F^{E_H}_{ab} + F^{E_R}_{ab}$. In our coordinates, it has the components:
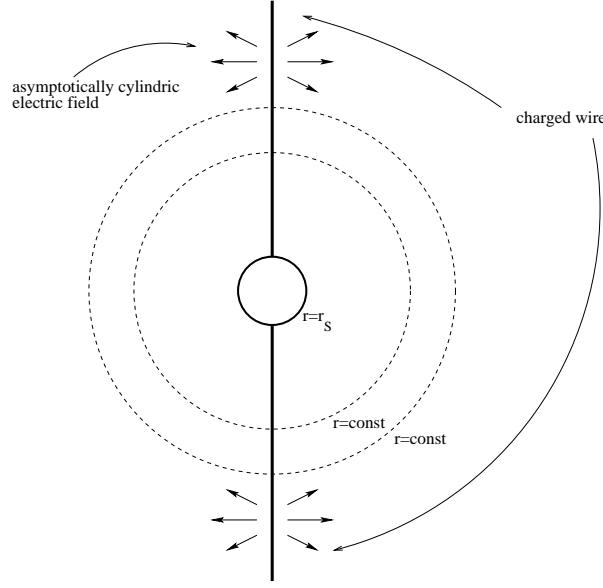
Figure 4. Illustration of the asymptotically cylindric electrostatic field of a uniformly charged wire suspended in a Schwarzschild spacetime. This field models the asymptotically horizontal electric field in an electrostatic or in a mixed magnetic-electric storage ring. The charge density of the wire can be determined by the charge integral under $r = $ const two-spheres, as described in the text. The free integration constants of such Maxwell fields are set so that the wire has uniform charge density in terms of r, and that under the sphere $r = r_S$ one has vanishing total charge.

$$F_{\mathsf{ab}}(t, r, \vartheta, \varphi) =$$

$$\begin{pmatrix} 0 & -E_R \frac{R^2}{r^2} & 0 & 0 \\ E_R \frac{R^2}{r^2} & 0 & 0 & -B \frac{r \sin^2 \vartheta}{\sqrt{1-\frac{r_S}{R}\left(\frac{L}{R}\right)^2}} \\ 0 & 0 & 0 & -B \frac{r^2 \sin \vartheta \cos \vartheta}{\sqrt{1-\frac{r_S}{R}\left(\frac{L}{R}\right)^2}} \\ 0 & B \frac{r \sin^2 \vartheta}{\sqrt{1-\frac{r_S}{R}\left(\frac{L}{R}\right)^2}} & B \frac{r^2 \sin \vartheta \cos \vartheta}{\sqrt{1-\frac{r_S}{R}\left(\frac{L}{R}\right)^2}} & 0 \end{pmatrix}$$

$$+ E_H \, L \, \mathcal{N}_{r_S} \begin{pmatrix} 0 & -\frac{1}{r}(1 + \frac{r_S}{r} \ln(\frac{1}{2} \sin \vartheta)) & -(1 - \frac{r_S}{r}) \frac{\cos \vartheta}{\sin \vartheta} & 0 \\ \frac{1}{r}(1 + \frac{r_S}{r} \ln(\frac{1}{2} \sin \vartheta)) & 0 & 0 & 0 \\ (1 - \frac{r_S}{r}) \frac{\cos \vartheta}{\sin \vartheta} & 0 & 0 & 0 \\ 0 & 0 & 0 & 0 \end{pmatrix}.$$

$$(60)$$

If the storage ring is purely magnetic, then $B \neq 0$, $E_H = 0$, $E_R \neq 0$, whereas for a purely electrostatic storage ring one has $B = 0$, $E_H \neq 0$, $E_R \neq 0$, while for a mixed magnetic-electric ring one has $B \neq 0$, $E_H \neq 0$, $E_R \neq 0$.

7. The absolute Larmor rotation in presence of electromagnetic fields

Whenever electromagnetic field is also present, the BMT equation, i.e., the second equation in Eq.(7), causes further rotation of the spin direction vector in addition to the Thomas rotation, the so-called *Larmor rotation.*

The beam motion is modelled by the cyclotronic worldline Eq.(2), and it has to satisfy the Newton equation, i.e., the first line of Eq.(7), against the field strength tensor Eq.(60). Given ω and E_H, that is fulfilled whenever the consistency conditions

$$
\begin{aligned}
B &= \omega \frac{m\,\gamma}{q} \sqrt{1 - \frac{r_S}{R}\left(\frac{L}{R}\right)^2} + \frac{E_H}{\omega\,L} \mathcal{N}_{r_S} \sqrt{1 - \frac{r_S}{R}} \sqrt{1 - \frac{r_S}{R}\left(\frac{L}{R}\right)^2}, \\
E_R &= \frac{r_S}{R} \frac{m\,\gamma}{2\,q\,R} \frac{1}{\sqrt{1 - \frac{r_S}{R}}} - E_H \frac{L}{R} \frac{r_S}{R} \mathcal{N}_{r_S}\left(1 + \ln\left(\frac{L}{2R}\right)\right)
\end{aligned}
\tag{61}
$$

hold with the notation $\gamma := \frac{1}{\sqrt{1 - \omega^2 L^2}}$. These are the equations of cyclotronic motion over a Schwarzschild background spacetime, with ω being the cyclotron circular frequency in terms of u_0-proper time. From this point on, it is assumed that Eq.(61) is satisfied, i.e., that the motion Eq.(2) of the particle is a consequence of a cyclotronic motion in electromagnetic field over a Schwarzschild spacetime. In the real g-2 and EDM experiments [4, 7] the magnetic field strength B and the horizontal electric field strength E_H are the fixed (measured) parameters, which determine ω and E_R, given the constants $\frac{m}{q}$, L, R, and the GR correction parameter $\frac{r_S}{R}$.

We are now at the point of evaluating the Larmor tensor $L_\omega{}^b{}_d :=$ $-\Lambda_\omega \frac{\mu}{s}\left(g^{bc}F_{cd} - u_\omega{}^b u_\omega{}^c F_{cd} - g^{bc}F_{ce}u_\omega{}^e u_\omega{}^f g_{fd}\right)$ which gives a contribution to the BMT equation, i.e., to the second line of Eq.(7). With that definition, the spin transport equation reads as

$$
\frac{\mathrm{d}}{\mathrm{d}t}\tilde{w}_\omega{}^{\mathsf{b}}(t) = \mathcal{F}_\omega{}^{\mathsf{b}}{}_{\mathsf{c}}\,\tilde{w}_\omega{}^{\mathsf{c}}(t) + L_\omega{}^{\mathsf{b}}{}_{\mathsf{c}}\,\tilde{w}_\omega{}^{\mathsf{c}}(t)
\tag{62}
$$

in terms of Killing time. In our coordinate conventions it has components as

$$L_\omega{}^b{}_d = -\frac{1}{2}\frac{g\,\omega\,\sqrt{1-\frac{r_S}{R}}}{1-\omega^2 L^2}$$

$$
\begin{pmatrix}
0 & -\omega L\frac{L}{R}\frac{\left(1-\frac{3}{2}\frac{r_S}{R}\right)}{\left(1-\frac{r_S}{R}\right)^{\frac{3}{2}}} & -\omega LR\frac{\sqrt{1-\left(\frac{L}{R}\right)^2}}{\left(1-\frac{r_S}{R}\right)^{\frac{1}{2}}} & 0 \\[2mm]
-\omega L\frac{L}{R}\left(1-\frac{3}{2}\frac{r_S}{R}\right)\left(1-\frac{r_S}{R}\right)^{\frac{1}{2}} & 0 & 0 & L\frac{L}{R}\left(1-\frac{3}{2}\frac{r_S}{R}\right) \\[2mm]
-\omega\frac{L}{R}\sqrt{1-\left(\frac{L}{R}\right)^2}\left(1-\frac{r_S}{R}\right)^{\frac{1}{2}} & 0 & 0 & \frac{L}{R}\sqrt{1-\left(\frac{L}{R}\right)^2} \\[2mm]
0 & -\frac{1}{R}\frac{\left(1-\frac{3}{2}\frac{r_S}{R}\right)}{\left(1-\frac{r_S}{R}\right)} & -\frac{R}{L}\sqrt{1-\left(\frac{L}{R}\right)^2} & 0
\end{pmatrix}
$$

$$-\frac{g\,q\,E_H\,\sqrt{1-\omega^2 L^2}}{2\,m\,\omega\,L}\,\mathcal{N}_{r_S}\left(1-\frac{r_S}{R}\right)^2$$

$$
\begin{pmatrix}
0 & -\omega L\frac{L}{R}\frac{1}{\left(1-\frac{r_S}{R}\right)^{\frac{3}{2}}} & -\omega LR\frac{\sqrt{1-\left(\frac{L}{R}\right)^2}}{\left(1-\frac{r_S}{R}\right)^{\frac{3}{2}}} & 0 \\[2mm]
-\omega L\frac{L}{R}\left(1-\frac{r_S}{R}\right)^{\frac{1}{2}} & 0 & 0 & L\frac{L}{R} \\[2mm]
-\omega\frac{L}{R}\frac{\sqrt{1-\left(\frac{L}{R}\right)^2}}{\left(1-\frac{r_S}{R}\right)^{\frac{1}{2}}} & 0 & 0 & \frac{L}{R}\frac{\sqrt{1-\left(\frac{L}{R}\right)^2}}{1-\frac{r_S}{R}} \\[2mm]
0 & -\frac{1}{R}\frac{1}{\left(1-\frac{r_S}{R}\right)} & -\frac{R}{L}\frac{\sqrt{1-\left(\frac{L}{R}\right)^2}}{1-\frac{r_S}{R}} & 0
\end{pmatrix}
$$

$$(63)$$

where the usual definition of the gyromagnetic factor $\mathbf{g} := \frac{2\,m\,\mu}{q\,s}$ was used. By construction, or by direct substitution it is seen that the tensor $L_\omega{}^a{}_b\,g^{bc}$ is antisymmetric, and therefore $L_\omega{}^a{}_b$ corresponds to a Lorentz transformation generator. Moreover, $L_\omega{}^a{}_b\,u_\omega{}^b = 0$ holds, which means that $L_\omega{}^a{}_b$ describes an $u_\omega{}^a$-rotation generator. That phenomenon is the *Larmor rotation*, and is an absolute, observer independent effect.

8. The relative Larmor precession as seen by the laboratory observer

Because of Eq.(62), according to the laboratory observer u_0, the spin direction vector $w_{\omega,u_0}{}^a$ satisfies the equation

$$\left(w_{\omega,u_0}{}^f\right)' = \Phi^T_{\omega,u_0}{}^f{}_b\,w_{\omega,u_0}{}^b + \Phi^L_{\omega,u_0}{}^f{}_b\,w_{\omega,u_0}{}^b, \tag{64}$$

with the definition $\Phi^L_{\omega,u_0}{}^f{}_b := \frac{1}{\Lambda_0}\,B_{u_0,u_\omega}{}^f{}_c\,L_\omega{}^c{}_a\,B_{u_\omega,u_0}{}^a{}_b$. By construction or by direct substitution it is seen that $\Phi^L_{\omega,u_0}{}^f{}_b\,g^{bc}$ is antisymmetric, which means that it describes a Lorentz transformation generator. Moreover, $\Phi^L_{\omega,u_0}{}^f{}_b\,u_0{}^b = 0$ holds, which means that it describes an u_0-rotation generator. The effect of $\Phi^L_{\omega,u_0}{}^f{}_b$ is called the *Larmor precession*.

In our coordinate conventions, it has the components

$$
\Phi^L_{\omega,u_0}{}^{\mathsf{a}}{}_{\mathsf{b}} = \begin{pmatrix}
0 & 0 & 0 & 0 \\
0 & 0 & 0 & \Phi^L_{\omega,u_0}{}^r{}_\varphi \\
0 & 0 & 0 & \Phi^L_{\omega,u_0}{}^\vartheta{}_\varphi \\
0 & \Phi^L_{\omega,u_0}{}^\varphi{}_r & \Phi^L_{\omega,u_0}{}^\varphi{}_\vartheta & 0
\end{pmatrix},
$$

with

$$
\Phi^L_{\omega,u_0}{}^\varphi{}_r = -\,\Phi^L_{\omega,u_0}{}^r{}_\varphi \, \frac{g^{\varphi\varphi}}{g^{rr}},
$$

$$
\Phi^L_{\omega,u_0}{}^\varphi{}_\vartheta = -\,\Phi^L_{\omega,u_0}{}^\vartheta{}_\varphi \, \frac{g^{\varphi\varphi}}{g^{\vartheta\vartheta}},
$$

$$
\Phi^L_{\omega,u_0}{}^r{}_\varphi = -\frac{1}{2}\,\mathsf{g}\,\omega\,L\,\gamma\,\frac{L}{R}\left(1 - \frac{3}{2}\frac{r_S}{R}\right) - \frac{\mathsf{g}\,q}{2\,m}\,\frac{E_H\,L\,\mathcal{N}_{r_S}\left(1-\frac{r_S}{R}\right)^{\frac{3}{2}}}{\omega\,R\,\gamma^2},
$$

$$
\Phi^L_{\omega,u_0}{}^\vartheta{}_\varphi = -\frac{1}{2}\,\mathsf{g}\,\omega\,\gamma\,\frac{L}{R}\sqrt{1 - \frac{L^2}{R^2}} - \frac{\mathsf{g}\,q}{2\,m}\,\frac{E_H\,\mathcal{N}_{r_S}\sqrt{1-\frac{r_S}{R}}}{\omega\,R\,\gamma^2}\sqrt{1 - \frac{L^2}{R^2}} \tag{65}
$$

with using the notation $\gamma := \frac{1}{\sqrt{1-\omega^2 L^2}}$.

The angular velocity vector of the Larmor precession can be obtained by the u_0 spatial Hodge dual of $\Phi^L_{\omega,u_0}{}^{\mathsf{a}}{}_{\mathsf{b}}$, according to the definition

$$
\Omega^L_{\omega,u_0}{}^{\mathsf{f}} := \frac{1}{2}\,u_0{}^{\mathsf{a}}\sqrt{-\det(g)}\,\epsilon_{\mathsf{abcd}}\,g^{\mathsf{bf}}\,\Phi^L_{\omega,u_0}{}^{\mathsf{c}}{}_{\mathsf{e}}\,g^{\mathsf{ed}}. \tag{66}
$$

Its components in our coordinate conventions are

$$
\Omega^L_{\omega,u_0}{}^{\mathsf{a}} = \begin{pmatrix}
0 \\
-\frac{1}{2}\,\mathsf{g}\,\omega\,\gamma\,\sqrt{1-\frac{L^2}{R^2}}\sqrt{1-\frac{r_S}{R}} - \frac{\mathsf{g}\,q}{2\,m}\,\frac{E_H\,\mathcal{N}_{r_S}\left(1-\frac{r_S}{R}\right)\sqrt{1-\frac{L^2}{R^2}}}{\omega\,L\,\gamma^2} \\
\frac{1}{2}\,\mathsf{g}\,\omega\,\gamma\,\frac{1}{R}\frac{L}{R}\frac{1-\frac{3}{2}\frac{r_S}{R}}{\sqrt{1-\frac{r_S}{R}}} + \frac{\mathsf{g}\,q}{2\,m}\,\frac{E_H\,\mathcal{N}_{r_S}\left(1-\frac{r_S}{R}\right)}{\omega\,R^2\,\gamma^2} \\
0
\end{pmatrix}. \tag{67}
$$

For charged particles in a cyclotronic motion, the total angular velocity vector of the spin precession is determined by $\Omega^S_{\omega,u_0}{}^{\mathsf{a}} := \Omega^T_{\omega,u_0}{}^{\mathsf{a}} + \Omega^L_{\omega,u_0}{}^{\mathsf{a}}$. Its components in our coordinate conventions are

$$
\Omega^S_{\omega,u_0}{}^{\mathsf{a}} = \begin{pmatrix}
0 \\
-\omega\left(1+\gamma\,a\right)\sqrt{1-\frac{r_S}{R}}\sqrt{1-\frac{L^2}{R^2}} - (1+a)\frac{E_H\,q\,\mathcal{N}_{r_S}\left(1-\frac{r_S}{R}\right)\sqrt{1-\frac{L^2}{R^2}}}{m\,\omega\,L\,\gamma^2} \\
\omega\,\frac{1}{R}\frac{L}{R}\left(\sqrt{1-\frac{r_S}{R}} + \gamma\,a\,\frac{1-\frac{3}{2}\frac{r_S}{R}}{\sqrt{1-\frac{r_S}{R}}}\right) + (1+a)\frac{E_H\,q\,\mathcal{N}_{r_S}\left(1-\frac{r_S}{R}\right)}{m\,\omega\,R^2\,\gamma^2} \\
0
\end{pmatrix}, \tag{68}
$$

where the usual notation $a := \frac{\mathsf{g}-2}{2}$ was used for the magnetic moment anomaly. The metric projections onto the orthonormal frame $\hat{r}^a$, $\hat{\vartheta}^a$, $\hat{\varphi}^a$ of $\Omega^S_{\omega,u_0}{}^{\mathsf{a}}$ are the followings:

$$-g_{ab}\,\hat{r}^a\,\Omega^S_{\omega,u_0}{}^b = -\omega\,(1+\gamma\,a)\sqrt{1-\frac{L^2}{R^2}} - (1+a)\frac{E_H\,q\,\mathcal{N}_{r_S}\,\left(1-\frac{r_S}{R}\right)^{\frac{1}{2}}\sqrt{1-\frac{L^2}{R^2}}}{m\,\omega\,L\,\gamma^2},$$

$$-g_{ab}\,\hat{\vartheta}^a\,\Omega^S_{\omega,u_0}{}^b = \omega\,\frac{L}{R}\left(\sqrt{1-\frac{r_S}{R}}+\gamma\,a\,\frac{1-\frac{3}{2}\frac{r_S}{R}}{\sqrt{1-\frac{r_S}{R}}}\right) + (1+a)\frac{E_H\,q\,\mathcal{N}_{r_S}\,\left(1-\frac{r_S}{R}\right)}{m\,\omega\,R\,\gamma^2},$$

$$-g_{ab}\,\hat{\varphi}^a\,\Omega^S_{\omega,u_0}{}^b = 0. \tag{69}$$

As discussed at the end of Section 4, the oscillation frequencies of the longitudinal and transverse spin component is determined by the length of the vector $\left(\Omega^S_{\omega,u_0} - \Omega^C_{\omega,u_0}\right)^a$. The coordinate components of that vector is given by

$$\left(\Omega^S_{\omega,u_0} - \Omega^C_{\omega,u_0}\right)^{\mathsf{a}} = \omega\,\gamma\,a\begin{pmatrix} 0 \\ -\left(1-\frac{r_S}{R}\right)^{\frac{1}{2}}\sqrt{1-\frac{L^2}{R^2}} \\ \frac{1}{R}\frac{L}{R}\frac{1-\frac{3}{2}\frac{r_S}{R}}{\left(1-\frac{r_S}{R}\right)^{\frac{1}{2}}} \\ 0 \end{pmatrix}$$

$$+(1+a)\frac{E_H\,q}{m\,\omega\,L\,\gamma^2}\begin{pmatrix} 0 \\ -\mathcal{N}_{r_S}\left(1-\frac{r_S}{R}\right)\sqrt{1-\frac{L^2}{R^2}} \\ \frac{1}{R}\frac{L}{R}\mathcal{N}_{r_S}\left(1-\frac{r_S}{R}\right) \\ 0 \end{pmatrix}. \tag{70}$$

Its metric projections onto $\hat{r}^a$, $\hat{\vartheta}^a$, $\hat{\varphi}^a$ is

$$-g_{ab}\,\hat{r}^a\left(\Omega^S_{\omega,u_0} - \Omega^C_{\omega,u_0}\right)^b = -\omega\,\gamma\,a\sqrt{1-\frac{L^2}{R^2}}$$
$$- (1+a)\frac{E_H\,q\,\mathcal{N}_{r_S}\,\left(1-\frac{r_S}{R}\right)^{\frac{1}{2}}}{m\,\omega\,L\,\gamma^2}\sqrt{1-\frac{L^2}{R^2}},$$

$$-g_{ab}\,\hat{\vartheta}^a\left(\Omega^S_{\omega,u_0} - \Omega^C_{\omega,u_0}\right)^b = \omega\,\gamma\,a\,\frac{L}{R}\frac{1-\frac{3}{2}\frac{r_S}{R}}{\left(1-\frac{r_S}{R}\right)^{\frac{1}{2}}}$$
$$+ (1+a)\frac{E_H\,q\,\mathcal{N}_{r_S}\,\left(1-\frac{r_S}{R}\right)}{m\,\omega\,L\,\gamma^2}\frac{L}{R},$$

$$-g_{ab}\,\hat{\varphi}^a\left(\Omega^S_{\omega,u_0} - \Omega^C_{\omega,u_0}\right)^b = 0. \tag{71}$$

In the g-2 experiments [4, 7], one has $B \neq 0$ and $E_H = 0$, i.e., purely magnetic storage ring is used, and the main observable is

$$\left|\Omega^S_{\omega,u_0} - \Omega^C_{\omega,u_0}\right| = |\omega\,a|\,\gamma\left(\left(1-\frac{L^2}{R^2}\right)+\frac{L^2}{R^2}\frac{(1-\frac{3}{2}\frac{r_S}{R})^2}{1-\frac{r_S}{R}}\right)^{\frac{1}{2}}. \tag{72}$$

It is seen, that GR gives slight contribution, the quantification of which is done in the following section.

In electric dipole moment (EDM) search experiments [12, 13, 14], the so called *frozen spin method* is used: the parameters B and E_H are adjusted such, that the vector $\left(\Omega^S_{\omega,u_0} - \Omega^C_{\omega,u_0}\right)^a$ vanishes to a best possible accuracy, and thus the observed spin direction vector is always exactly tangential to the orbit, i.e., points in the direction

$\hat{\varphi}^a$. If an EDM of the particle would exist, it manifests as a residual precession, out of the orbital plane. The identities Eq.(61) and Eq.(70) tell us that in the Minkowski limit ($r_S = 0$), the frozen spin condition is quite possible to achieve via setting $E_H = -\frac{a}{1+a}\frac{m}{q}L\omega^2\gamma^3$, assuming that the magnetic anomaly a of the particle was measured in advance. In the GR case, however, the complete vanishing of $\left(\Omega^S_{\omega,u_0} - \Omega^C_{\omega,u_0}\right)^a$ is not possible to achieve exactly, and at best the frozen spin condition can only be achieved approximately. For instance, one may require that the vertical projection $-g_{ab}\,\hat{v}^a\left(\Omega^S_{\omega,u_0} - \Omega^C_{\omega,u_0}\right)^b$ vanishes, which is fulfilled whenever

$$E_H = -\frac{a}{1+a}\frac{m}{q}L\omega^2\gamma^3\frac{1}{\mathcal{N}_{r_S}\left(1-\frac{r_S}{R}\right)^{\frac{1}{2}}}\frac{1-\frac{3}{2}\frac{r_S}{R}\frac{L^2}{R^2}}{1-\frac{r_S}{R}\frac{L^2}{R^2}} \tag{73}$$

holds, as seen from Eq.(70). In that case, there will be a residual precession out of the orbital plane, with magnitude

$$\left|\Omega^S_{\omega,u_0} - \Omega^C_{\omega,u_0}\right| = |\omega\,a|\,\gamma\frac{1}{2}\frac{r_S}{R}\frac{L}{R}\left(1-\frac{r_S}{R}\right)^{-\frac{1}{2}}\frac{\sqrt{1-\frac{L^2}{R^2}}}{\sqrt{1-\frac{r_S}{R}\frac{L^2}{R^2}}} \tag{74}$$

and the direction of the precession is upward vertical whenever $-\omega\,a$ is positive, and downward vertical otherwise. The magnitude of this GR correction to a frozen spin scenario is quantified in the next section.

9. Evaluation of the GR corrections to Thomas plus Larmor precession

First, the effect of GR is evaluated on the cyclotron frequency ω. This frequency is uniquely determined by the first line of Eq.(61), given the vertical magnetic field strength B and the horizontal electric field strength E_H of the storage ring, and the constants $\frac{m}{q}$, L, R, along with the GR correction parameter $\frac{r_S}{R}$. In order to determine the r_S dependence of ω, it should be regarded as an implicit function of r_S. Its first order GR correction is nothing but its first Taylor expansion term in terms of r_S, and that can be easily derived by differentiating against r_S the pertinent consistency equation between ω, B and E_H. It follows that one has

$$r_S\left(\frac{\mathrm{d}}{\mathrm{d}r_S}\omega\bigg|_{r_S=0}\right) = \omega\frac{1}{2}\frac{r_S}{R}\frac{L^2}{R^2}\frac{1-\frac{1}{\gamma^2}+\frac{2E_H q L\left(1+\ln\left(\frac{L}{2R}\right)\right)}{m\gamma}}{\gamma^2-1-\frac{E_H q L}{m\gamma}}. \tag{75}$$

The last quotient expression is ≈ 1 for relativistic particles, and thus the relative error of ω caused by the neglection of GR is $\approx\frac{1}{2}\frac{r_S}{R}\frac{L^2}{R^2}$, which is of the order of 10^{-21}, as already quantified in Section 5. Therefore, that correction is pretty much negligible for current and foreseeable experimental applications. One could also say, that in the system there are two small parameters: $\frac{r_S}{R}$ and $\frac{L}{R}$, and the corrections of the third order, such as $\frac{r_S}{R}\frac{L^2}{R^2}$, are considered to be negligible. That also means that in the GR correction estimations, the r_S dependence of ω can be neglected in order to simplify the formulas.

As a next step, the effect of GR on the main observable of the muon g-2 experiments [4, 7] is evaluated, which is the frequency of the longitudinal spin projection. That was

shown equal to the quantity $\left|\Omega^S_{\omega,u_0} - \Omega^C_{\omega,u_0}\right|$, which was shown to take the form Eq.(72) in a purely magnetic g-2 ring ($B \neq 0$, $E_H = 0$). In the Minkowski limit, this has its well known special relativistic form

$$\left|\Omega^S_{\omega,u_0} - \Omega^C_{\omega,u_0}\right|\Big|_{r_S=0} = |\omega\, a|\, \gamma, \tag{76}$$

which is the principal formula for g-2 determination. Its first order Taylor expansion term in terms of r_S is seen to be

$$r_S\left(\frac{\mathrm{d}}{\mathrm{d}r_S}\left|\Omega^S_{\omega,u_0} - \Omega^C_{\omega,u_0}\right|\Big|_{r_S=0}\right) = -|\omega\, a|\,\gamma\,\frac{r_S}{R}\frac{L^2}{R^2}, \tag{77}$$

causing a relative systematic error of $-\frac{r_S}{R}\frac{L^2}{R^2}$, being negligible, of the order of $-2\cdot 10^{-21}$. Therefore, that correction is negligible for current g-2 experimental applications. (For simplicity, the tiny r_S dependent correction of ω, quantified in Eq.(75), was neglected in the formula.)

The first apparent sizable GR correction can be seen in the total spin precession vector $\Omega^S_{\omega,u_0}{}^a$. Namely, whenever one uses a purely magnetic storage ring ($B \neq 0$, $E_H = 0$) with a particle with magnetic anomaly $-1 < a < 0$, such as deuteron nuclei which do have $a \approx -0.142$ [38], then there exists a unique velocity (or B) setting for which $1 + a\,\gamma = 0$ holds. As seen from Eq.(69), in that case the spin precession vector $\Omega^S_{\omega,u_0}{}^a$ vanishes in the Minkowski limit ($r_S = 0$), meaning that the spin direction vector is merely parallel transported in the space of the laboratory observer. One could call such a scenario a "*zero torque setting*". In the GR case, however, a small approximately horizontal component of $\Omega^S_{\omega,u_0}{}^a$ persists, of the magnitude $\left|\Omega^S_{\omega,u_0}\right| = \left|\omega\frac{L}{R}\left(\sqrt{1-\frac{r_S}{R}} - \frac{1-\frac{3}{2}\frac{r_S}{R}}{\sqrt{1-\frac{r_S}{R}}}\right)\right|$, as seen from Eq.(69). Taking its first Taylor term in r_S, this is of the magnitude $\beta\frac{r_S}{2R^2}$ with the notation $\beta := \omega\, L$, being the circular velocity in units of speed of light. When translated to ordinary units from the used geometric units, this is nothing but $\beta\frac{\mathbf{g}}{c}$ with $\mathbf{g}$ denoting the gravitational acceleration on the Earth's surface, and c denoting the speed of light. This residual precession quantifies as $\approx 3.26 \cdot 10^{-8}$ rad/sec if one assumes a deuteron beam, which shall satisfy $1 + a\,\gamma = 0$ at $\beta \approx 0.9804$. In such a configuration with an initially tangential spin vector, the spin will not merely be parallelly transported as in the Minkowski limit, but it will tilt in and out of the orbital plane. The amplitude of this vertical polarization buildup is, however, too small to experimentally measure. That is because the spin vector is not approximately perpendicular to the residual $\Omega^S_{\omega,u_0}{}^a$ vector at all times, and thus the polarization does not accumulate with elapsing time. That issue can be remedied with an experimental setting discussed below.

The GR correction is expected to have a measurable effect on *frozen spin experiments*, such as EDM search experiments [12, 13, 14]. For these settings, in the Minkowski limit, the spin direction vector always follows the tangent of the orbit curve, i.e., $\left(\Omega^S_{\omega,u_0} - \Omega^C_{\omega,u_0}\right)^a\Big|_{r_S=0} = 0$ holds. In case of GR, there are no such parameter settings when this frozen spin condition holds, but as indicated previously, one may can choose

a setting in which case the vertical projection of the vector $\left(\Omega^S_{\omega,u_0} - \Omega^C_{\omega,u_0}\right)^a$ vanishes. In that case, the residual precession shall elevate the spin direction vector out of the orbital plane, with a rate Eq.(74). Again, in order to quantify that, we take its first Taylor expansion term in terms of r_S, which is

$$r_S \left(\frac{\mathrm{d}}{\mathrm{d}r_S} \left|\Omega^S_{\omega,u_0} - \Omega^C_{\omega,u_0}\right| \bigg|_{r_S=0} \right) = |\omega\,a|\,\gamma\,\frac{1}{2}\frac{r_S}{R}\frac{L}{R}\sqrt{1 - \frac{L^2}{R^2}}. \tag{78}$$

Taking into account that $\frac{L}{R} \ll 1$ and $\beta = \omega L$, this quantifies as $|a\,\beta\gamma|\frac{r_S}{2R^2}$. When translated from the geometric units to normal units, it corresponds to the expression

$$|a\,\beta\gamma|\frac{\mathbf{g}}{c} \tag{79}$$

which quantifies as $\approx |a\,\beta\gamma|\,3.26\cdot10^{-8}\,\mathrm{rad/sec}$.§ Thus, in this setting, given an initially longitudinally polarized beam, a vertical polarization buildup will be seen at the rate of $\left|\Omega^S_{\omega,u_0} - \Omega^C_{\omega,u_0}\right| \approx |a\,\beta\gamma|\,32.6\,\mathrm{nrad/sec}$, as shown in Fig. 5. This magnitude of polarization buildup rate is well within the experimental reach for the planned EDM experiments [12, 13, 14], since the spin coherence of e.g. proton beams can be maintained for about an hour with today's beam technology. Therefore, we propose to use the foreseen *frozen spin* or EDM experiment also as sensitive GR experiments on spin propagation. Although the fake EDM signal by GR is much larger than an expected true EDM signal, they are distinguishable due to their opposite sign flip behavior for a change of the beam circulation direction, i.e., due to their opposite chirality behavior.

10. Concluding remarks

In this paper, a fully general relativistic calculation was performed in order to evaluate the GR corrections over a Schwarzschild background for particle spin precession experiments, such as the muon g-2 measurement [4] or the electric dipole moment (EDM) search experiments [12, 13, 14]. It turns out that although GR gives a first order correction in r_S for certain important observables, its contribution to the muon g-2 measurements is negligible. That is because in that setting spin precession in the horizontal plane is studied, and GR mainly gives contribution to the other direction, moreover the amount of precession due to the g-2 signal is large anyway. However, for

§ Our formula Eq.(79) is also in accordance with the post-Newtonian approximative results of [21], which was obtained for the special case of a purely electrostatic ($B = 0$, $E_H \neq 0$) frozen spin storage ring. In such a ring, the Newton equation Eq.(61) and the frozen spin condition Eq.(73) as well as the zero magnetic field condition $B = 0$ needs to be satisfied at the same time, in the $r_S = 0$ limit. That is only possible for particles with $a > 0$, and also singles out a so-called *magic momentum* $\beta\gamma = \frac{1}{\sqrt{a}}$ which is necessary in order to satisfy all these conditions. The residual vertical precession due to GR contribution is seen in that special case to be $\sqrt{a}\,\frac{\mathbf{g}}{c}$, by means of Eq.(79), which confirms the calculation of [21]. It is seen, however, that using a mixed magnetic-electric frozen spin storage ring might be more advantageous, since it can be applied to any a, and does not single out a small value for the Lorentz factor γ. Indeed, via using large γ, the GR effect can be arbitrarily magnified. Therefore, for a specific GR experiment, we propose to use a mixed magnetic-electric frozen spin ring, with as large γ as possible, and particles with large a.
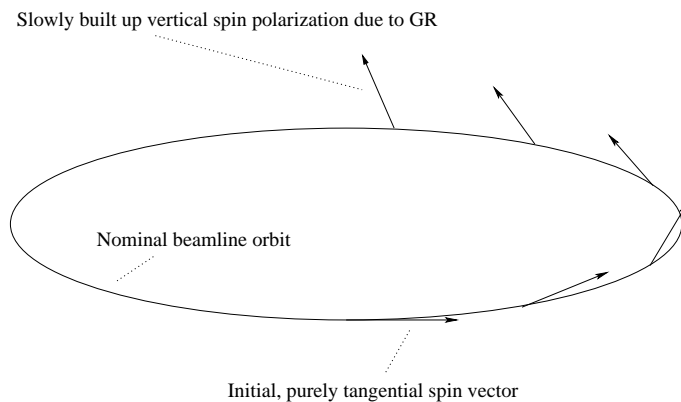
Figure 5. Illustration of the effect of GR corrections to a frozen spin setting. The GR correction results in a slow buildup of vertical spin polarization, if the beam was initially longitudinally polarized. The rate of the polarization buildup is given by Eq.(79).

EDM search experiments, in which case a so-called frozen spin situation is obtained with a combination of the γ factor and of the electric and magnetic fields, the GR effects imitate a fake EDM signal. That is a precession out of the orbital plane, of the magnitude $|a\,\beta\gamma|\,\mathbf{g}/c$, being of the order of $3.26 \cdot 10^{-8}$ rad/sec, which is well above the planned sensitivity of $\approx 10^{-9}$ rad/sec of these experiments, and pretty much above the Standard Model (SM) expectation. Thus, the EDM experiments provide a unique platform for experimental test of GR in terms of particle spin propagation. Moreover, in any frozen spin experiment with aimed precision not worse than 10^{-6} rad/sec, the GR signal needs to be subtracted in order to access any signature coming from particle physics — SM or BSM. Fortunately, direct experimental elimination of such backgrounds may also be achieved by comparing the effect as seen from normally and reversely rotating beams, since the GR effect would change sign, but the EDM effect would not [12, 13, 14]. If such subtraction is done, the GR signal is expected to be distinguishable from a real EDM signal and vice versa.

Acknowledgments

References

[1] T. Morishima, T. Futamase, H. M. Shimizu: *The general relativistic effects on the magnetic moment in Earth's gravity*; Prog. Theor. Exp. Phys. **2018** (2018) 063B07 [`arXiv:1801.10244`].

[2] T. Morishima, T. Futamase, H. M. Shimizu: *Post-Newtonian effects of Dirac particle in curved spacetime - II : the electron g-2 in the Earth's gravity*; [`arXiv:1801.10245`].

[3] T. Morishima, T. Futamase, H. M. Shimizu: *Post-Newtonian effects of Dirac particle in curved spacetime - III : the muon g-2 in the Earth's gravity*; [`arXiv:1801.10246`].

[4] The Muon g-2 experiment [`http://muon-g-2.fnal.gov`].

[5] G. W. Bennett et al: *Final report of the E821 muon anomalous magnetic moment measurement at BNL*; Phys. Rev. D **73** (2006) 072003 [`arXiv:hep-ex/0602035`].

[6] J. P. Miller, E. de Rafael, B. L. Roberts: *Muon (g-2): Experiment and Theory*; Rept. Prog. Phys. **70** (2007) 795 [`arXiv:hep-ph/0703049`].

[7] S. R. Mane, Y. M. Shatunov, K. Yokoya: *Spin-polarized charged particle beams in high-energy accelerators*; Rept. Prog. Phys. **68** (2005) 1997.

[8] M. Visser: *Post-Newtonian particle physics in curved spacetime*; [`arXiv:1802.00651`].

[9] P. Guzowski: *The effect of Earth's gravitational field on the muon magic momentum*; [`arXiv:1802.01120`].

[10] H. Nikolic: *Can effective muon g-2 depend on the gravitational potential?*; [`arXiv:1802.04025`].

[11] C. Lämmerzahl, G. Neugebauer: *The Lense-Thirring Effect: From the Basic Notions to the Observed Effects*; In: C Lämmerzahl, C. W. F. Everitt, F. W. Hehl (eds) Gyros, Clocks, Interferometers: Testing Relativistic Graviy in Space, Lecture Notes in Physics, vol 562 Springer (2001).

[12] Y. Senichev et al: *Quasi-frozen spin concept of deuteron storage ring as an instrument to search for electric dipole moment*; Proceedings of IPAC2017 (2017) TUPVA084, 2275.

[13] Y. Semertzidis: *Storage ring EDM experiments*; Eur. Phys. J. Web. Conf. **118** (2016) 01032.

[14] R. Talman: *The Electric Dipole Moment Challenge*; IOP Concise Physics (2017).

[15] Gravity Probe B experiment [`https://einstein.stanford.edu`].

[16] C. W. F. Everitt et al: *Gravity Probe B: Final Results of a Space Experiment to Test General Relativity*; Phys. Rev. Lett. **106** (2011) 221101 [`arXiv:1105.3456`].

[17] A. Kobach: *Gravitational effects on measurements of the muon dipole moments*; Nucl. Phys. **B911** (2016) 206 [`arXiv:1603.00127`].

[18] A. J. Silenko, O. V. Terayev: *Equivalence principle and experimental tests of gravitational spin effects*; Phys. Rev. **D76** (2007) 061101 [`arXiv:gr-qc/0612103`].

[19] Y. N. Obukov, A. J. Silenko, O. V. Terayev: *Manifestations of the rotation and gravity of the Earth in high-energy physics experiments*; Phys. Rev. **D94** (2016) 044019 [`arXiv:1608.03808`].

[20] Y. N. Obukov, A. J. Silenko, O. V. Terayev: *Manifestations of the rotation and gravity of the Earth in spin physics experiments*; Int. J. Mod. Phys. **A31** (2016) 1645030.

[21] Y. Orlov, E. Flanagan, Y. Semertzidis: *Spin rotation by Earth's gravitational field in a "frozen-spin" ring*; Phys. Lett. **A376** (2012) 2822.

[22] S. Hawking, G. F. R. Ellis: *Large Scale Structure of Spacetime*; Cambridge University Press (1973).

[23] R. M. Wald: *General Relativity*; Chicago University Press (1984).

[24] M. Conte, R. Jagannathan, S. A. Khan, M. Pusterla: *Beam optics of the Dirac particle with anomalous magnetic moment*; Particle Accelerators **56** (1996) 99.

[25] J. D. Jackson: *Classical Electrodynamics*; Wiley (1999).

[26] M. Mathisson: *Neue Mechanik materieller Systeme*; Acta. Phys. Polon. **6** (1937) 163.

[27] A. Papapetrou: *Equations of motion in general relativity*; Proc. Phys. Soc. **64** (1951) 57.

[28] W. G. Dixon: *A Covariant Multipole Formalism for Extended Test Bodies in General Relativity*; Nouvo Cimento **34** (1964) 317.

[29] W. G. Dixon: *Classical theory of charged particles with spin and the classical limit of the Dirac equation*; Nuovo Cimento **38** (1965) 1616.

[30] A. A. Deriglazov, W. G. Ramírez: *Recent progress on the description of relativistic spin: vector model of spinning particle and rotating body with gravimagnetic moment in General Relativity*; Adv. Math. Phys. **2017** (2017) 7397159 [`arXiv:1710.07135`].

[31] F. A. E. Pirani: *On the Physical significance of the Riemann tensor*; Acta Phys. Polon. **15** (1956) 389.

[32] W. M. Tulczyjew: *Motion of multipole particles in general relativity theory*; Acta Phys. Polon. **18** (1959) 393.

[33] W. Rindler: *Relativity: Special, General, and Cosmological*; Oxford University Press (2006).

[34] T. Matolcsi, M. Matolcsi, T. Tasnádi: *On the relation of Thomas rotation and angular velocity of reference frames*; Gen. Rel. Grav. **39** (2007) 413 [`arXiv:math-ph/0611047`].

[35] GRTensorII [`http://grtensor.phy.queensu.ca`].

[36] R. S. Hanni, R. Ruffini: *Schwarzschild black hole in an asymptotically uniform magnetic field*; Lett. Nuovo Cimento **15** (1976) 189.

[37] L. Binet: *Electrostatics and magnetostatics in the Schwarzschild metric*; J. Phys. **A9** (1976) 1081.

[38] N. J. Stone: *Table of nuclear magnetic dipole and electric quadrupole moments*; Atomic Data and Nuclear Data Tables **90** (2005) 75.